T-violation detection in "elastic" *pp* scattering in a single beam FIGURE-8 collider

Richard M Talman
Laboratory for Elementary Particle Physics, Cornell University, Ithaca, NY, USA
(Dated: September 27, 2022)

In a Derbenev-style figure-8 storage ring, independently polarized, diametrically opposite bunches of a single beam collide at the crossing point. This makes it practical to investigate spin dependence and time reversal T-symmetry of "elastic" *pp* scattering with unprecedented sensitivity. Recognizing that the proton is anomalous, e.g. anomalous MDM, "elastic" scattering may be accompanied by T-violating spin rearrangement with undetectably small energy excitation. Operating above the 69.5 MeV laboratory energy at which proton-carbon scattering asymmetry analyzing power exceeds 99% to roughly 400 MeV (the pion production threshold), both scattered protons come to rest in graphite polarimeter chambers providing nearly full directional coverage. Both initial proton polarization states are pure and both final state proton polarizations are measured with nearly ideal analyzing power.

The presence or absence of T-violation in nuclear forces is thought to bear significantly on important cosmological issues, especially missing mass, dark energy, and the matter/anti-matter imbalance. The possible existence of a semi-strong, T-violating, nuclear force with coupling strength compatable to the electromagnetic interaction was proposed independently by Lee and Wolfenstein, by Prentki and Veltman, and by Okun in 1965.

Unlike fixed target experiments, rather than being collinear, in Derbenov geometry incident beams collide at right angles. All initial and final state laboratory proton energies being equal produces a huge statistical polarimetric advantage. *Persuasive visual evidence of T-violation will be provided by unexpected correlation between the p-carbon scattering directions of final state protons.*

Spin dependence is most easily detectable at low proton energy. Rearrangement of existing COSY components into a "FIGURE-8" storage ring allows diametrically opposite polarized proton bunches in a single stored beam to collide. "Spin transparency" in figure-8 geometry is used to enable Fourier enhancement of T-violation sensitivity.

The required COSY lab rearrangement is also compatable with PTR, a prototype EDM measurement ring capable of measuring the deuteron anomalous MDM using easily achievable, superimposed electric and magnetic bending.

Of the uncertain properties of nuclear physics, none is more fundamental than nucleon, nucleon interaction. A "toy" theoretical model incorporating the anomalous proton EDM predicts strong T-violation; the Derbenov collider configuration promises its unambiguous detection.

CONTENTS

I. INTRODUCTION

This paper is a companion to two papers with related subject matter [1][2].

Derbenev et al.[3] have demonstrated theoretically the practicality of measuring scattering cross sections at the crossing point of figure-8 storage rings. A solitary stored beam "collides with itself" in the sense that diametrically-opposite bunches automatically pass through each other in synchronism at the intersection point (IP) where the beam crosses itself.

This paper describes experiments to investigate possible violation of time reversal invariance (T-violation) in the form of finite EDMs or in "elastic" *pp* scattering, where the quotation marks acknowledges the possibility of collisions for which the energy dissipation is undetectably small. The possible existence of a semi-strong, symmetry-violating nuclear force with coupling strength comparable to the electromagnetic interaction was proposed by Lee and Wolfenstein[4], by Prentki and Veltman[5], and by Okun[6][7] in 1965.

Accepting the Derbenev accelerator physics analysis of orbit and spin evolution, including "spin transparency", a figure-8 storage ring having polarimetry with nearly full 4π acceptance, and analyzing power ranging from 80% to 100% over substantial solid angular range is described. As well as enabling Fourier statistical enhancement of symmetry violation in *pp* scattering, spin transparency allows the same figure-8 ring to be used for deuteron EDM measurement.

1. Modern spin control; ancient nuclear physics

In 1950, when 20 MeV was "high energy physics", nuclear EDMs were thought to play a significant role in the photo-dissociation of nuclei such as the deuteron. This physics is explained in Section XII-E of Morse and Feshbach[8]. The inferred value of the deuteron EDM at that time, as quoted by Gamow's Table I[9], expressed as a photo-dissociation cross section was $2.7e^{-27}\,\mathrm{cm}^2$. For some reason the presence of what seems to be violation of time reversal (T) symmetry seems to have been forgotten. Perhaps Norman Ramsey's surprise concerning a non-zero EDM effect provided some of his motivation for initiating his program to measure the neutron EDM? But subsequent measurements have provided only upper limits for the neutron EDM.

The present paper suggests that the nucleon dipole moment prototype complex, PTR + BA (bunch accumulator) be designed to be easily and inexpensively convertable[1] back and forth, with the "FIGURE-8" storage ring, capable of detecting T-violation in *pp*-scattering and/or by measuring the deuteron EDM, as well as other electric and magnetic dipole moments.

The energy region emphasized in this paper, "above" Rutherford scattering, "below" meson threshold, is paradoxical in various ways. Quoting Alice, (in Wonderland) the behavior becomes "curiouser and curiouser", the more it is investigated. Total *pp* cross sections are plotted at the top in Figure 1, which is copied from a heroic 1993 review by Lechanoine-LeLuc and F. Lehar, [11], containing seven pages of references, from an era in which a large experimental group had five members.

Though originally mysterious, the complicated long wavelength behavior (i.e. low energy region below, say, 100 MeV) quickly became well understood in terms of interference between Rutherford and nuclear amplitudes. The same cannot be said for the short wavelength, higher energy region, above, say, 500 MeV, where inelastic scattering quickly becomes dominant. Spin dependent *pp*

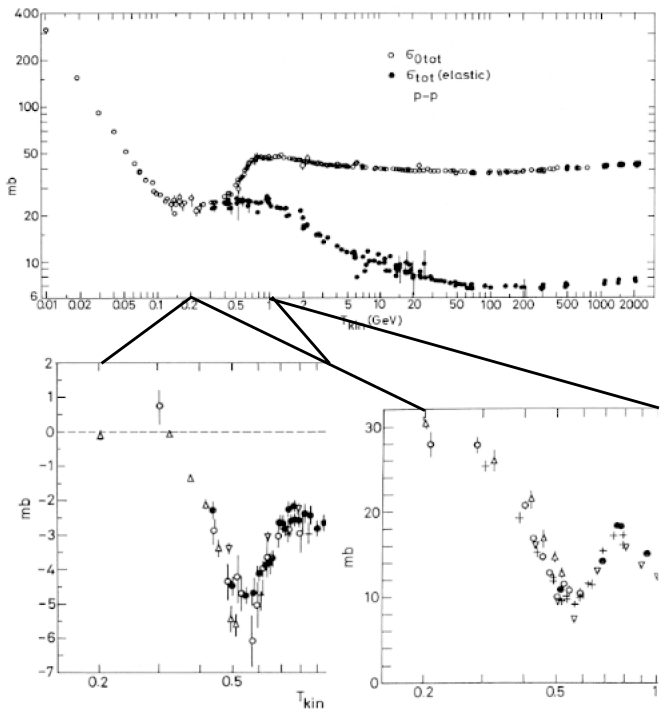

FIG. 1. (Copied from reference [11]) **Above:** Energy dependence of *pp* spin-independent total cross section (open circles) and total elastic cross section (solid curves). **Below left:** $\sigma_{1tot}(pp) = -(1/2)\Delta\sigma_T(pp)$ transverse spin energy dependence, **Below right:** $-\Delta\sigma_L(pp)$ longitudinal spin energy dependence.

cross sections, measured with polarized beams and polarized hydrogen target are plotted at the bottom of Figure 1. The sudden onset of this strong polarization dependent resonance suggests that the energy range of the *pp* measurement proposed in the present paper should be extended to, for example, 800 MeV.

Certainly the pure initial spin states, the near-ideal po-

[1] More realistically, with "easily" including several month shutdown, and "inexpensively" poorly defined, what is being proposed, is to keep several options open until more detailed designs have been produced.

larimetry plus the particle tracking capability will enable identification and interpretation of the inelastic channels accounting for this resonance. This option would, however, entail higher energy protons. To avoid further complication, this option is not pursued in the present paper.

From an experimentalist's kinematic planning perspective, from the *pp* elastic scattering cross section simplification given by Eqs. (10) and (11) in Section III, this energy range could scarcely be more boring—the scattering is isotropic and the total cross section is constant.

It seems curious, therefore, that the error bars and the scatter of values in this region are some five times greater than at almost any other region of the plot. Though not at all suggested by this plot, an empirical, partial wave fit at the center of the region, at 310 Mev, based on data available in 1965[12], required 12 non-vanishing partial waves, when the isotropy observed in coarse early experiments suggested that just 1 or 2 might be expected.

Of all nuclear processes it might initially have been expected that understanding elastic *pp* scattering would be assigned highest priority. And, based on counting the number of PhD theses implied by the seven pages of reference mentioned above, this effort was strongly supported for several decades. Yet, it seems fair to say that *pp* elastic scattering is still not understood in any fundamental sense.

We choose to explain this paradoxical history by the combination of the strong influence of proton spins along with the feeble experimental capability to control the initial spin states and the near total inability to measure the final spin states. Since the angular momentum associated with the spins of fundamental particles is still so mysterious, it should perhaps not be surprising that partial wave analysis, which is based on conservation of angular momentum, is so impotent.

The present proposal claims to rectify both of these defects. Technology now available enables the preparation of pure initial spin states along with nearly ideal final state measurement of both final spin states. *To be consistent with the huge investment in this area in the past one expects, therefore, significant support for these measurements in the present.*

There is at least one exception to the statement made previously that *pp* scattering is not understood in any fundamental sense.[2] It is the so-called Gerosimov-Drell-Hearn sum rule[13][14], which connects static properties of the nucleon—like the anomalous magnetic moment and the nucleon mass—with an integration from zero to infinity, of a difference of spin dependent doubly polarized total absorption cross sections of real photons. Quoting from Helbing[15]"The experimental data verify the GDH Sum Rule for the proton at the level of 8% including the systematic uncertainties from extrapolations to unmeasured energy regions." Based purely on sound field theory, this surely qualifies as "some kind of understanding in a fundamental sense".

As it happens, a peripheral capability of the apparatus we propose is the capability of precise measurement of MDMs of the nuclei of many low mass isotopes, stable or weakly unstable, to which other sum rules might apply. Since the proton MDM is already known to 11 decimal places, it must not be claimed that this MDM capability is required to evaluate the right hand side of the GDH sum rule. Neither may it be claimed to contribute to the integrand on the left hand.

What may be hoped for from the GDH sum rule is better understanding of the paradoxical *pp* interaction behavior under discussion. From a qualitative perspective, one anticipates an improved theoretical understanding of how cross sections well outside our narrow energy range can help to understand seemingly paradoxical elastic *pp* scattering.

A paper by Bystricky, Lehar and Winternetz [10] provides a detailed breakdown of *pp* and *pd* scattering amplitudes, with special concentration on time reversal invariance (TRI). The paper by Lechanoine-LeLuc and Lehar [11], whose importance has already been emphasized, reviews the voluminous nucleon-nucleon elastic scattering data, including polarization, with analyses, as of 1993, from well below to well above the energy range considered in the present paper, up to a few GeV

Vastly more powerful experimental tools are available today than in the past. This is especially true of the precision spin control techniques that have been developed at the COSY laboratory in Juelich Germany[16][17][18][19][20][21].

The so-called "exchange force", postulated initially by Heisenberg, later revised by Wigner and others, models the dependence on the same spins that control the polarizations of elastic nucleon scattering. Along with the importance of exchange forces in fitting the binding energies of all nuclei from A=1 to A=200, it was the assumption of time reversal (T) conservation that constrained this modeling. Then till now, other than its theoretical elegance, there has been no persuasive experimental evidence, one way or the other, for requiring T-conservation of the nuclear force.

With the anticipated EDM statistical precision inversely proportional to the square root of run duration in mind, it has, until recently, been assumed that run duration times would be limited by the spin coherence time (SCT). Recent developments[22] have suggested that this is not the case. Run durations in excess of 1000 s, (a conventionally-adopted design goal) are now thought to be allowed by lattice design optimized for the cancellation of sources of polarization decoherence.

A more important, and unavoidable, consideration limiting run durations, is now thought to come from the consumption of beam particles associated with the destructive polarization measurements needed for phase locking the beam spin tunes[22]. It is this capability that permits

[2] The following digression into the GDH sum rule is the result of numerous conversations between the author and Kolya Nikoliev.

electric and magnetic fields to be repeatably set, reliably reversed, and reset, without the need for (unachievably precise) electric and magnetic field measurement. The ability to precisely reverse beam circulation directions provides powerful capability for reducing systematic error by averaging over beam revolution reversals. This has lowered the priority associated with requiring two beams to counter-circulate simultaneously rather than consecutively.

These considerations have motivated, in the present paper, the re-ordering of PTR prototype ring development sequencing from the ordering defined initially in the CERN Yellow Report (CYR)[23]. Development of the superimposed electric and magnetic sector bends needed for PTR can proceed "in parallel" with the construction of the FIGURE-8 ring and with the construction of the polarimetric tracking chamber needed for *pp* scattering measurement, and applicable as well to EDM measurement; all with the common goal of investigating time reversal symmetry. Spin transparency allows the same figure-8 ring to be used for deuteron EDM measurement. See Section VI 3.

2. Investigation of the strong nuclear force

The present paper is intended to provide support also for the gradual implementation of PTR facility planned at COSY as prototype for eventual frozen spin deuteron and proton EDM measurement, with the same purpose, of investigating T-reversal symmetry.

With co-author Kolya Nikolaev, a Snowmass 2021 presentation[24] describes how a prototype EDM ring (such as described in the present paper) can be used to investigate the physics goal of detecting beyond standard model (BSM) *semi-strong T-violation in elastic pp or pd scattering.*

In τ-θ puzzle days (late 50's to mid-60's) such a mechanism was suggested independently by Lee & Wolfenstein[4], by Prentki & Veltman[5], and by Okun[6][7][25]. Other, similarly motivated, conjectures have been numerous. Search for such a medium-strength, T-violating nuclear force provided the initial motivation for this paper.

Much earlier, elementary particle physicists had concentrated on low energy *pp*, *pn*, and *pd* scattering measurement and theory, with the view of understanding the nuclear forces responsible for nuclear scattering. Starting from the work of Heisenberg, Wigner and, later, Gamow, Bethe, and others, exchange forces had been adjusted and partial wave models had been produced and tested. The following few paragraphs have been extracted almost verbatim from Mott and Massey[26]

Especially influential were the "scalar" Wolfenstein operators, for primary beam particle "1" incident secondary target particle "2";

$$\mathbf{1},\quad \boldsymbol{\sigma}_1\cdot\boldsymbol{\sigma}_2,\quad (\boldsymbol{\sigma}_1+\boldsymbol{\sigma}_2).\boldsymbol{n},\quad (\boldsymbol{\sigma}_1-\boldsymbol{\sigma}_2).\boldsymbol{n},$$

$$(\boldsymbol{\sigma}_1\cdot\boldsymbol{p})(\boldsymbol{\sigma}_2\cdot\mathbf{p}),\quad (\boldsymbol{\sigma_1}\cdot\boldsymbol{n})(\boldsymbol{\sigma_2}\cdot\mathbf{n}),\quad (\boldsymbol{\sigma_1}\cdot\boldsymbol{q})(\boldsymbol{\sigma_2}\cdot\mathbf{q})$$

where "**1**" is the identity matrix, and the three components of the $\boldsymbol{\sigma}_1$ and $\boldsymbol{\sigma}_2$ "vectors" are the three Pauli 2x2 matrices. As shown in Fig. 2, orthonormal coordinate basis vector $\mathbf{n}$ is an axial unit pseudo-vector which, with orthogonal incident momentum unit vectors $\mathbf{p}$ and $\mathbf{q}$, defines the scattering plane, to which $\mathbf{n}$ is orthogonal. These are the possible forms in terms of which the scattering matrix can be composed and matched phenomenologically with measured values at each value of beam energy.

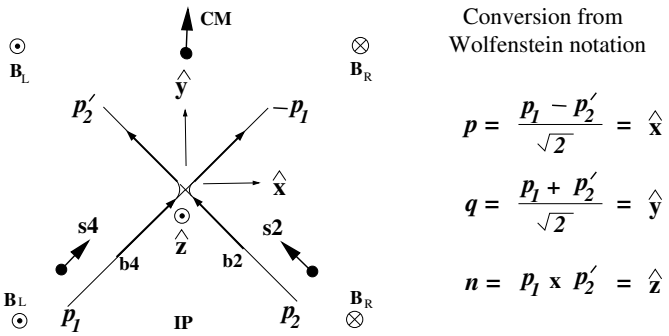

FIG. 2. For orthogonal Derbenev mode beam collisions the Wolfenstein incident momentum unit vectors $\mathbf{p}$ and $\mathbf{q}$, along with normal to the scattering plane $\mathbf{n}=\mathbf{p}\times\mathbf{q}$, become Cartesian unit vectors $\hat{\mathbf{x}}$, $\hat{\mathbf{y}}$, $\hat{\mathbf{z}}$. The $\mathbf{B_L}$ and $\mathbf{B_R}$ symbols can only be understood in connection with Fig. 3.

Already formidably complicated, two Wolfenstein "pseudo-scalar" forms,

$$(\boldsymbol{\sigma}_1\times\boldsymbol{\sigma}_2)\cdot\boldsymbol{n},\ \text{and}\qquad (\boldsymbol{\sigma}_1\cdot\boldsymbol{p})(\sigma_2\cdot\boldsymbol{q})+(\boldsymbol{\sigma}_1\cdot\boldsymbol{q})(\sigma_2\cdot\boldsymbol{p}) \tag{1}$$

have (conventionally) been excluded on the basis that they violate T-reversal and/or P-symmetry.

Based on this phenomenological formulation, a description of nuclear forces capable of accurately accounting for the parameters of all nuclei and for the decay of all unstable nuclear isotopes was gradually established. A substantial portion of this understanding was based on the treatment of protons as elementary particles for which there was no relevant concept of "binding energy" required. Binding energies were defined relative to the proton binding energy (taken to to be zero). In detail, the exchange force was taken to be a best compromise of Heisenberg, Wigner and Majorana exchange force variants, based on measured binding energies.

By τ-θ puzzle days, the elementary particle community had "moved on" from what had by then become "low energy" nuclear physics, accepting, with little subsequent alteration, the existing phenomenologic description of the force between nucleons. Note, however, that there has been little other than theoretical prejudice for requiring time reversal symmetry conservation.

In the meantime Gell-Mann quarks had been introduced as constituents of the proton. This made protons composite, contrary to adopted modeling that treats the proton as elementary. Logically, its composite nature might reasonably have been accompanied by the possibility of the proton itself having binding energy[3].

There is thought to be a close connection between time reversal (T-symmetry) and the baryon/anti-baryon imbalance in our present day universe. This connection was stressed by Sakharov[28] in an early and influential paper. Nowadays, to a first approximation, our universe contains only protons. One has to suppose that the laws of particle physics are consistent with symmetry-breaking processes which have resulted in a surplus of what we now call protons. As Sakharov famously explained, any generation of such an imbalance of particles and anti-particles required statistical disequilibrium conditions, absence of baryon number conservation, and CP- (and hence also T-) violation in one or more of the fundamental laws of particle production and decay.

Building on the Wolfenstein formulation, traditional analyses, after having dropped the T-violating operators, have proceeded to "simplify" the algebra by proceeding to a density matrix formulation. This approach assumes implicitly that every experimental apparatus would be limited in ways that would require summation over initial state amplitudes and/or averaging over final state amplitudes.

The fact that the Pauli operators are 2x2 matrices already make it difficult to acquire any simple intuitive correlation between momenta, on the one hand, and separation into spin-flip and non-spin-flip events on the other. Density matrix formulation makes this algebraically achievable, but intuitively opaque.

For the detection apparatus proposed here, since there is no need for the summing or averaging of amplitudes, introduction of density matrix formulation is unnecessary. The explicit isolation of T-violating and T-conserving amplitudes makes the basic Wolfenstein formulation especially appropriate.

II. ORTHOGONAL COLLISIONS OF PAIRED BUNCHES IN A SINGLE BEAM FIGURE-EIGHT STORAGE RING

1. Orthogonal beam scattering coordinates

The proposed figure-8 storage ring is shown schematically in Figures 3 and 6. Though intended to serve as a measurement of elastic scattering, the experiment commences by treating the apparatus as two matched polarimeters being "calibrated" in coincidence. A single beam contains four bunches, $\mathbf{b_1}$, $\mathbf{b_2}$, $\mathbf{b_3}$, and $\mathbf{b_4}$, with individually controlled polarizations $\mathbf{s_1}$, $\mathbf{s_2}$, $\mathbf{s_3}$, and $\mathbf{s_4}$. Fig. 3 shows bunches $\mathbf{b_2}$, and $\mathbf{b_4}$ about to collide at the intersection point (IP). More detailed ring representations are shown in subsequent figures.

It is implicit in the Wolfenstein operator definitions for the incident beams to be collinear. In our application the incident beams are orthogonal in the laboratory reference frame, and therefore not quite orthogonal in the CM frame, which is shown moving upward in Fig. 2. Our configuration, which resembles Wolfenstein's t-channel, is shown with time advancing directly up the page.

The CM velocity is not very large in the laboratory, and significant CM symmetry is preserved because of the transversely symmetric orthogonal approach of the incident beams in the laboratory. Though the protons approach at right angles in the lab, in the CM frame the approach is collinear, as are the scattered trajectories.

The corresponding laboratory frame constraint is that incident and scattered momenta pairs are orthogonal, and all four energies are identical. In the laboratory, as well as defining a (horizontal) plane, the incident trajectories define a $\pm\pi/2$ "right-angle cone", centered on the transverse axis along which the CM is traveling. The scattered trajectories necessarily lie on the other branch of the same cone, necessarily orthogonal also, and defining a plane containing the same conical axis but, in general, skew to the horizontal plane, by some non-zero azimuthal angle Φ.

With the incident particle momenta defining a circle on the cone of incidence, the scattered particle momenta lie on the mirror-symmetric circle on the other branch of the cone. As a consequence, the scattered particle trajectories are also orthogonal in the laboratory with identical energies, the same as the incident particle energies. *It is their equal energies that permit both scattered particle polarizations to be measured with nearly perfect 100% analyzing powers.*

Wolfenstein's incident particle momenta are $\mathbf{p_1}$ and $\mathbf{p_2}$, and scattered particle momenta are $\mathbf{p'_1}$ and $\mathbf{p'_2}$. Our incident particles $\mathbf{p_1}$ and $\mathbf{p_2}$ are his $\mathbf{p1}$ and $-\mathbf{p'_2}$. Fig. 2 includes translation formulas on the right for conversion back to Wolfenstein's basis vector definitions.

So far it is only the $\mathbf{b_2}, \mathbf{b_4}$ bunch pairing that has been discussed. Of course, the same discussion applies to the $\mathbf{b_1}, \mathbf{b_3}$ bunch pairing. During bunch polarization preparation each of the four bunch polarizations can be prepared arbitrarily. This makes it convenient to compare the different outcomes from differently prepared incident states merely by maintaining the separation of "even bunch index" and "odd bunch index" incident bunch pairs.

[3] In a paper introducing integer charge quarks, Han and Nambu[27] suggested implicitly the influence on binding energies, but, with "color" persuasively introduced, this seems not to have been pursued.

PTR OPERATION as POLARIZED p,p COLLIDER

ALL COSY INJECTION , BEAM AND SPIN CONTROL IS PRESERVED
THERE IS NO ACCUMULATING EDM SIGNAL
BEAM HAS VANISHING SPIN TUNE
POLARIMETER: 0.9 < A < 1.0 EFFICIENCY ~ 0.002

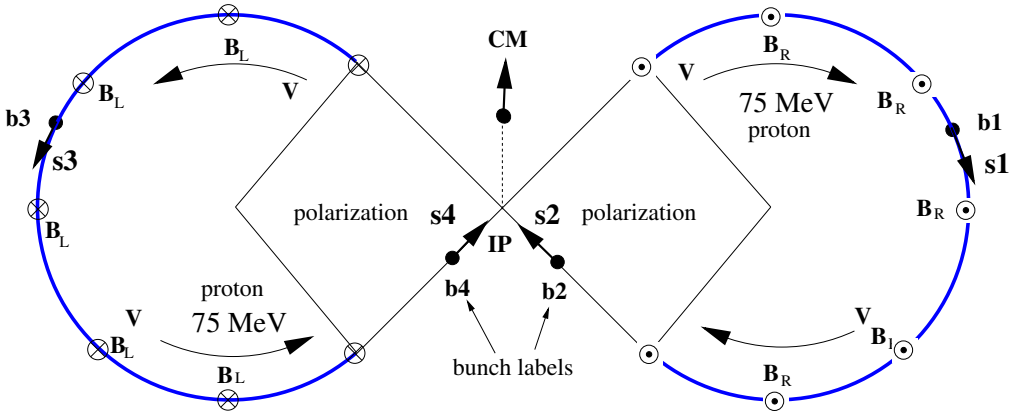

FIG. 3. Conversion of COSY for PTR implementation as a polarized *pp* collider. Since the spin tune vanishes ($Q_s = 0$) bunch polarizations can be set independently and can be phase locked (shown pointing forward as **s2** and **s4** for bunches **b2** and **b4**) to remain frozen indefinitely. *Two beams cannot counter-circulate at the same time.* But beam circulation direction can be reversed with frequency domain setting and re-setting precision, without the need for (impractically precise) electric and magnetic field measurement. This is almost as useful as simultaneous counter-circulation for reducing significant systematic errors by averaging over reversals. Both incident beam spins states at the collision intersection point (IP) can be pure, and each scattered particle momentum and polarization are measured with maximum possible (100%) analyzing power as each it slows through 69.5 MeV energy.

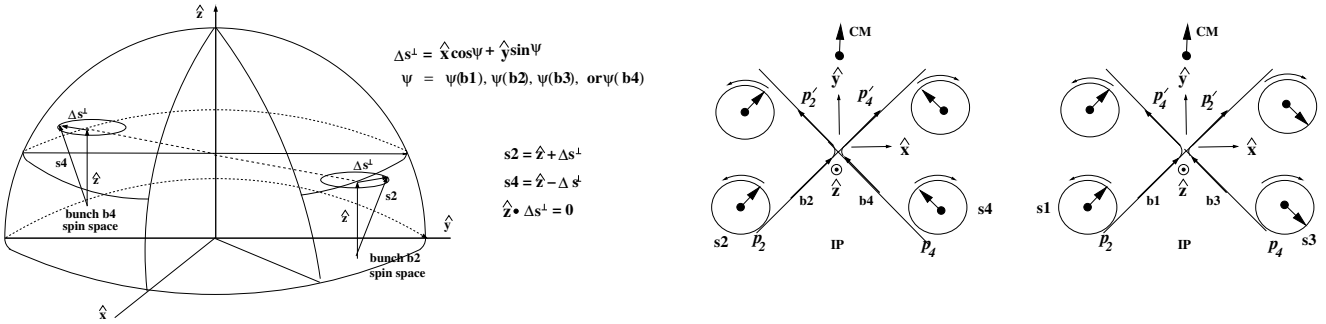

FIG. 4. Exploiting adiabatic spin transparency, beam spin orientations can be scanned coherently, for example to achieve Fourier series statistical enhancement of T-violation detection sensitivity; see Section VI 2 1. **Left:** Two of four beam bunch spins are shown. Colliding pairs are **b1**,**b3** and **b2**,**b4**. Phase angles ψ are externally controllable independently for each of the four beam bunches. **Right:** Spins of bunches **b1** and **b2** are the same, **b3** and **b4** opposite.

2. Achievement of near perfect analyzing power

Nearly perfect analyzing power is less impressive (but no less essential) than it seems. As a proton slows down, its analyzing power exceeds 0.99 only briefly. However the analyzing power remains greater than 0.9 for an appreciable fraction of the proton's full range. Since the scattered proton energies are identical in the laboratory, the beam energy does not need to be much greater than 69.5 MeV, for all scattered energies to exceed the energy at which the graphite analyzing power exceeds 99%. Also graphite chamber thickness great enough to stop all scatters is easily achieved, irrespective of scattering angle. See Fig. 8 and Table V.

The polarization of every proton scattered at the IP, and scattered again in one of the near crystalline graphite foil (or construction grade graphene) plates of the detection chamber, will have been determined with unprece-

dented accuracy, irrespective of scattered proton direction. This will provide high quality positive elastic signature for every elastic scatter. The total stopping ranges of every proton, including weakly inelastic scatters, will be used to reject inelastic scatters.

With such cleanly matched pairs of elastic scatters, the comparison of time-forward and (effectively) time-reversed scatters can be performed with unprecedented accuracy on an event by event basis. For example, the equality of scattering probability P and analyzing power A (required to be equal by time reversal symmetry) can be checked for matched pairs of protons. Furthermore, (with sufficient incident spin orientation control) by altering the incident pure polarization states, the reversed-time version of any observed forward-time scatter can be re-created. In other words, truly forward-time and backward-time scatters can be compared.

Preparation of two or more deuteron bunches in individualized spin states as assumed in this paper, could be demonstrated immediately at COSY, using the methods described in reference [21].

3. A proton as "toy" storage ring electric bend

In a *pp* colliding beam situation one can think of the proton in beam 1 as the incident particle and the proton in beam 2 as the "target". Why not, instead, think of the target proton as an electric bend element in a (tiny, Fermi-scale) circular storage ring? Here this ring will be referred to as a "toy proton storage ring". Approximate parameters for such a storage ring are given in Table I. Because the electric force is repulsive, the bend elements would have to be situated on a circle outside the storage ring orbit. Parameters for such a "toy storage ring" are given in Table I. Though the orbits are actually parabolic, for sufficiently small bend angle each truncated arc is more or less circular.

Similar looking parameter tables are given for rings of practical storage rings of various bending ratio, as large as 100 m bending radius to as small as 10 m, are contained in references [1] and [2]. The bending radius of our toy storage ring is 10^{-15} m. Curiously, other than (very small) sizes, and (very large) electric fields, the magnitudes seem familiar. In particular, the spin tune $Q_s^E \equiv$" QsE1 is typical of any storage ring. As a consequence one expects significant precession of in-plane components of proton spin. Though the spins have negligible effect on particle motion, electromagnetic fields have strong influence on the spin orientations. The quantitative implications of are discussed in this section, even if it seems to make little sense to discuss nuclear force divorced from electromagnetic force. It can be interesting to try to understand in detail how completely electromagetism overpowers nuclear symmetry. As small as the proton is, experimental realities require any proton field to be effectively uniform. Even with highly polarized beams there can be a strong tendency for symmetry violating ampitudes to cancel

Time reversal symmetry of a nuclear collision is said to require that, if one spin flips, so also must the other. The nuclear force between two colliding protons is capable of causing spin flips but, to simplify , it will be assumed to begin with that the the nuclear force conserves both spin states.

A major contention of the present paper is that previous experimental tests of the spin-flip consistency required by time rversal symmetry, have not adequately accounted for the influence of the anomalous MDM of the proton. It is claimed here that the effect of the proton anomolous m is to convert perfect spin-flip consistency into nearly maximal spin-flip inconsistency. If true, the proposed experiment will unambiguously demonstrate strong T-violation.

The role of proton MDM must, therefore, be analysed. As two protons approach, both are are in known pure initial spin states, and the only significant force fields are their repulsive electric fields. Superficially, the absence of magnetic field suggests the constancy of both spin states. But this is not true since, in the proton rest frames, there are non-vanishing magnetic fields that cause the spins to precess at a rate corresponding to their electric spin tunes, Q^E.

Copying from reference [2], the spin tune in a purely electric ring is given by

$$Q_s^E = G\gamma - \frac{G+1}{\gamma}, \tag{2}$$

where γ is the usual relativistic factor, and G is the anomalous MDM, whose value for the proton is $G_p = 1.7928474$. For a circulating proton with spin pointing forward at time $t = 0$, the spin-forward probability is,

$$P = \frac{1}{2}\left(1 + \cos(2\pi n_t Q_s^E)\right) \tag{3}$$

where turn number n_t is an integer only for complete turns around the ring.

Even in the absence of nuclear force, as a result of their near encounter, the final proton spin states differ from the inital spin states. The remainder of this subsection shows that this electric-induced spin precession masks any purely-nuclear T-conservation constraint. Stated differently, since electric and nuclear fields are married so inseparably in every nucleus, one must conlude that, on an event by event basis, any T-symmetry constraint imposed by purely nuclear force is over-ridden by the effect of anomalous MDM.

Table I provides parameters for our toy storage ring. This table resembles similar tables in references [1][2]. (Though not germane to the present discussion) calculations associated with this table also solve for a case in which superimposed electric and magnetic fields are adjusted such that the proton 1 spin tune is globally frozen and such that proton 2 would counter circulate on the same orbit. The electric and magnetic bendin fields are

constructive for 49.90 MeV protons in beam 1 and destructive for 39.06 MeV in beam 2. In our case, where there is no magnetic field, the spin tune is given in the table as QsE1=-0.7636, which is the spin tune for our toy proton ring.[4] [5]

Previous tests of T-violation have involved summing or averaging over states which can , potentially, produce insignificant cummulative T-violation, in spite of the fact that T-violation (along with P-violation, and failure of angular momentum conservation) is approximately maximal on an event by event basis. The present section analyzes this possibility quantitatively.

One sees from Figure 3 that our "toy storage ring proton element" would bend a stored proton beam through exactly 90 degrees, or $2\pi/4$. One concludes that the local spin precession angular advance is 0.7636. Notice, however, that this precession advance applies only to the component of incident proton spin that lies in the scattering plane. The out-of-plane component of proton 1 suffers no precession. For simpliciity we ignore this consideration, since it adds complexity without much influencing quantitative measures of T-violation.

Empirically, at the kinetic energies under discussion, elastic *pp* scattering is quite accurately isotropic; see Eq. (10). It is customarily accepted that, in *pp* scattering, it is impossible to associate an individual scattered proton with a particlar incident proton. Yet, from Figure 3, one sees that the incident proton on the left is the scattered proton observed on the left—it would be observed on the right only if it had (in effect) not scattered at the IP.

A purely nuclear interaction, with anomalous moment precession neglected, might have left both final states purely polarized, perhaps parallel. From Eq. (4) one sees that the anomalous MDM effect would result in proton 1 remaining in its not-flipped state with probability,

$$P = \frac{1}{2}\left(1 + \cos(2\pi n_t Q_s^E)\right) \approx 0.5 \neq 1. \qquad (4)$$

and the same for proton 2. Because 90 degrees in the laboratory is not the same as 90 degrees in the center of mass, more work is needed to conplete this estimate.

III. LOW ENERGY *pp* ELASTIC SCATTERING SEARCH FOR TIME-REVERSAL VIOLATION

1. Detection apparatus

The goal of the proposed scattering experiment is to reduce, by a large factor, elastic scattering *pp* T-violating upper limits, currently roughly one percent. This would use highly polarized beams in the figure-eight storage ring being described in the present paper for colliding beam elastic scattering measurement. Even though some electric bending will eventually be required for EDM measurement using PTR, initially the bending will be all-magnetic.

Magnetic fields are opposite in the two partial rings making up the figure-eight bending. Counter-circulating beams are not required. Diametrically opposite bunches, such as **b2** and **b4**, collide at intersection point IP, at the center of the cross-over line.

An important role of RF acceleration (which is not shown, and which necessarily averages to zero) is to phase lock the beam revolution frequency to an extremely accurate absolute frequency over long runs. A possibly more important role is one which will require the quite high RF frequency required to prepare the short bunch lengths that will be needed to achieve high luminosity. If there is an "Achilles's' heel" to the present proposal, this is it.

The plan is to measure below-pion-threshold elastic *pp* (or *dd*) scattering in (fixed-target-equivalent) $150 < E < 400$ MeV range. This would exploit the JEDI-Juelich-developed [23] long spin coherence time, spin phase-locked, pure spin-state, polarized beam technology.

Final-state, single-particle polarization measurements are sensitive to T-violation in double-spin observables. For the goal of detecting T-violation in (measurably) elastic *pp* (or *dd*) scattering, the detection chamber shown in Fig. 7 is located at the intersection point (IP) of the figure-8 ring. Kinematic characteristics of protons stopping in graphite are exhibited in Appendix B. The proposed tracking chambers are up-down (or left-right as appropriate) symmetric, with nearly full 4π solid angle detection, except for the vertically-central section which is heavily compromised by the requirement that the colliding beams are crossing at right angles.

Final state detection will be provided for nearly every elastic *pp* scatter, by stopping both scattered particles in coincidence in the up-down (or left-right) symmetric, polarization-sensitive, tracking chambers. With nearly full acceptance, high-efficiency polarimetry is provided for every elastic *pp* scatter.

Description of this capability is especially simple since, unlike scattering from a target fixed in the laboratory, the storage ring frame of reference is close to the CM frame. The negligible spread of stopping energies makes it practical to study the full stopping tracks of both scattered particles for every scatter. This "clean" scattering detection provides a substantial advantage for colliding beam measurement compared to fixed target measurement. Here "clean" particle detection means two unambiguous single tracks detected in time-coincidence, with accurately valid kinematics. Final state proton energies will be equal, which can be expected to provide sensitive elastic/inelastic selectivity. These events will provide accurate spin-dependent differential cross section measurements over most of 4π steradians.

[4] One might complain that, because of the relative motion of beams 1 and 2, there would be a Liénard-Wichert magnetic effect as well, but this deflection is negligible.

[5] The sign of QsE1 is negative, meaning that the proton spin precesses less rapidly than the proton momentum, which expressed as a "precession rate", would correspond to $Q_{\mathrm{momentum}} = 1.0$.

beam1	m1	G1	q1	beta1	K1	E0rho	QsE1	m2	G2	q2	beta2	KE2	bratio	QsE2	beam2
	GeV				MeV	MV						MeV			
	r_0 =		$1.0e^{-15}$ m =		1.0 Fermi	"**Toy**"	**ring**								
p	0.9383	1.7928	1	0.31377	49.9039	86.3327	-0.7636	0.9383	1.7928	1	-0.27989	39.0610	-0.89201	-0.81	p

TABLE I. A "target" proton can be treated as if it is an electric bending element in a "toy" storage ring with bending radius of, say, 1 Fermi. One sees from this table that a 49.9 MeV proton would sense the (full ring) spin tune to be $QsE1 = -0.7636$, as calculated from Eq. (2).

bm	m1	G1	q1	etaE1	p1c/q1	E0	B0	m2	G2	q2	etaE2	p2c/q2	bratio	Qs2	bm
1	GeV				GeV	MV/m	mT	GeV				GeV			2
	r_0 =	95 m													
d	1.8756	-0.1430	1	-0.17243	0.3432	-0.1253	4.7341	1.8756	-0.1430	1	0.52631	-0.0447	-0.13237	-5.93955e-01	d
d	1.8756	-0.1430	1	-0.17243	0.3432	-0.1253	4.7341	1.8756	-0.1430	1	-0.17243	0.3432	1	-4.00000e-15	d

TABLE II. (Table, with caption revised, from reference[2]) showing kinetic parameters for counter-circulating deuteron beams in a tunnel with 95.5 m bending radius, matching the AGS tunnel, for which the circumference is 809 m. These deuteron rows are typical of almost all atomic nuclei for which only one or the other beam can have vanishing spin tune. For simultaneous counter-circulation the kinematic beam conditions are especially hard to meet in the deuteron case because the ratio, "bratio", of frozen spin beam velocities, like the ratio of momenta, is so different from unity. As an aside, one notes though, because of the large radius of the AGS tunnel, that all electric and magnetic field values are conveniently small.

Colliding beam luminosity calculations and collision rate estimates are covered in Appendix C. Based, as they are, on luminosity formulas that apply to head-on collisions, these formulas probably over-estimate the luminosity of right angle collisions. From this perspective, our assumed rates have probably been over-estimates. *Until realistic transfer line optics and realistic longitudinal beam dynamics has been established, the absolute rates used in this paper are not very reliable.* One can say, alternatively, that the run durations required to obtain the assumed numbers of scattering events is uncertain.

Other considerations are also important. As well as enabling high beam polarizations, electron cooling inherited from COSY will reduce beam emittances, and energy spreads. From this perspective, our assumed rates have been under-estimates.

With roughly one in 400 tracks scattering elastically in a polarimetry tracking chamber, 10^6 events are expected to exhibit at least one elastic p-carbon scatter. With both incident beams nearly 100% up-polarized, these million events are candidates for potential detection of spin flips forbidden by T-symmetry. These are optimal events in the sense that a substantial fraction are subject to polarimetric analyzing power averaging greater than 90%.

Persuasive visualization of T-violation will be provided by unexpected correlation between the azimuthal scattering directions of coincident final state protons upon their entry to the tracking chambers, where the analyzing powers are close to 100%. When all events are distributed by their (precisely-known) energies, their distributions in energy must match the dependence of analyzing power on energy, which is close to 100% for tracks starting close to the entrance to the chamber. As a result the events carrying most of the statistical information are the "early scatters" occurring shortly after chamber entrance. This makes it sensible to tally up-down and left-right polarization determinations layer by layer in the tracking chambers. In other words, efficiencies and analyzing powers can be evaluated layer by layer, with events sorted into corresponding bins.

Of the 10^6 events just discussed, roughly 2500 will show two clean polarization sensitive scatters. Events with both tracks starting close to the chamber entrance will be "gold-plated" in the sense that both scattered particle spin states have been measured with high analyzing power, meaning that their spin state, "up" or "down" is known with near certainty. Of course, these will represent only a quite small fraction of the double-scatter events, but their statistical weight will be huge.

So far the distributions have been assumed to contain no T-violating scatters. One sees, already, the need for quite complicated data processing, in order to identify T-violating events. One therefore seeks initial spin state preparation that can be expected to maximize the fraction of events that are good candidates for counting as evidence of T- or P-violation[6].

Investigation to be spelled out next, has produced the initial spin state preparation shown in Fig. 4.

2. Forbidden "null detection" of T-violation

Because of CPT symmetry, which is usually assumed to be sacrosanct, a violation of CP-symmetry is equivalent to a violation of T-symmetry. Though CP violation of the weak nuclear force has been observed, this violation seems too weak to account for the imbalance of matter and anti-matter in the present day universe. Current

[6] The discussion will continue to be ambivalent as to the separate identification of T- and P-violation. Since charge conjugation plays no obvious role in pp scattering, it is hard to avoid invoking PCT conservation, which would imply that any T-violation has to be canceled by a P- violation.

bm	m1	G1	q1	beta1	K1	E0	B0	m2	G2	q2	beta2	KE2	bratio	Qs2	bm
1	GeV				MeV	MV/m	mT	GeV				MeV			2
	$r_0 = 11.0\,\mathrm{m}$														
d	1.8756	-0.1430	1	0.18000	31.1438	-0.9684	36.5816	1.8756	-0.1430	1	-0.02383	0.5326	-0.13237	-5.93955e-01	d
d	1.8756	-0.1430	1	0.18000	31.1438	-0.9684	36.5816	1.8756	-0.1430	1	0.18000	31.1438	1	-3.00000e-15	d

TABLE III. Differing from Table II primarily by reducing bending radius from $r_0 = 95\,\mathrm{m}$ to $r_0 = 11.0\,\mathrm{m}$, this table exhibits the quite low value of the electric field value, $E0 = -0.9684\,\mathrm{MV/m}$, superimposed on also weak magnetic $B0 = 36.58\,\mathrm{mT}$ needed to freeze the global deuteron spin tune, $Q_s = 0$. These parameters are appropriate for BA+PTR operation in the COSY beam hall.

models have both strong interaction and electromagnetic interactions preserving P and T symmetry individually. Since charge conjugation plays no role in elastic nuclear scattering, CPT-conservation reduces to PT violation for nuclear scattering, such as the elastic *pp* or *dd* scattering under discussion. This does not make the detection of P-violation and T-violation equivalent, however, for various reasons.

Though weak (by definition) the weak nuclear force can be expected to play some role in elastic *pp* or *dd* scattering. So the detection of P-violation, *per se*, would be of less interest than the detection of T-violation. More important, and considered next, is the fact that there are significant theory-based limitations to the extraction of T-violation from experimental measurement of scattering rates.

This issue was introduced by Arash, Moravcsik and Goldstein[29] who showed that, independent of dynamical assumptions, no "null T-violation experiment" could be designed. Here a "null experiment" experiment is defined to mean any experiment for which a statistically significant non-vanishing observed counting rate would demonstrate time reversal violation.

Before commencing their proof, these authors usefully define three classes of symmetry-violation detection experiment: (i) performing sequentially, an experiment followed by "theoretically the same" experiment run backwards in time; (ii) measuring a "self-conjugate" reaction which, under time reversal, goes into the same reaction; and (iii) a null experiment, as defined in the previous paragraph. The authors cite experiments of type (iii) that set fractional upper limits on parity-violation as small as 10^{-7}. The simplest example of type (i) is the time-reversal scattering requirement for polarization P in a forward scattering process to be equal to analyzing power A in the time-reversed process.

Arash et al. point out the necessity of significantly different apparatus for type (i) counting rate comparisons, and (correctly, from this experimentalist's point of view) of an inevitable uncertainty in matching the acceptance apertures of two diverse experiments to an accuracy very much better than 1 percent. It becomes increasingly difficult to reduce violation upper limits by an increasingly large factor.

Arash et al. proceed to prove the impossibility of designing a null experiment capable of detecting T-violation. Taken together, their arguments present a bleak future for direct experimental detection of T-violation. This section reviews the Arash et al. results. A later section describes the extent to which our proposed storage ring experiment circumvents some of their detailed conclusions without contradicting their acknowledged validity.

A predicate for the Arash, Moravcsik and Goldstein (mathematically abstract) proof is that measurable polarized state scattering rates are due exclusively to bilinear combinations of scattering amplitudes. They do, however, acknowledge that "there is one relationship that circumvents this constraint, *namely the optical theorem*, (based on probability conservation) in which a rate bilinear in amplitudes is related to a rate linear in intensities, although only in a special way (namely, utilization of the real part of the forward reaction amplitude)."

Arash et al., also mention a proposal of Stodolsky[30] who had earlier pointed out the same "loop-hole" by suggesting an "interesting time reversal test with polarized targets" by measuring slow neutron-nuclei forward scattering.

Quoting Stodolsky almost verbatim, for spin vectors of neutron and target respectively, he
"imagines (beam polarizations) $\mathbf{s}_n$ and $\mathbf{s}_T$ to be at right angles to each other, and to the *beam direction* $\mathbf{m}$. Then, to restore the original direction, he performs a 180° around, say, the $\mathbf{s}_n$ axis, which reverses the direction of $\mathbf{s}_T$. Thus time-reversal invariance requires

$$F_{\mathbf{s_n}x,\mathbf{s_T}y} = F_{\mathbf{s_n}x,-\mathbf{s_T}y} \tag{5}$$

where x and y are meant to show that $\mathbf{s}_n$ and $\mathbf{s}_T$ are oriented perpendicular to each other, and to the beam axis z. In other words, detection of time-reversal violation favors regions centered where

$$F \sim (\mathbf{s}_n \times \mathbf{s}_T) \cdot \mathbf{m} \quad . \tag{6}$$

is maximal[7]

Stodolsky continues by suggesting theoretically plausible sources of such a term in the forward scattering amplitude. Though useful for a neutral particle such as the neutron, for charged particles, Rutherford scattering,

[7] Since the condition expressed in Eq. (6) was derived assuming collinear incident beams, its application in the current situation is murky, other than suggesting that, for sensitivity to symmetry violation, nether spin direction should be parallel to either incident beam direction.

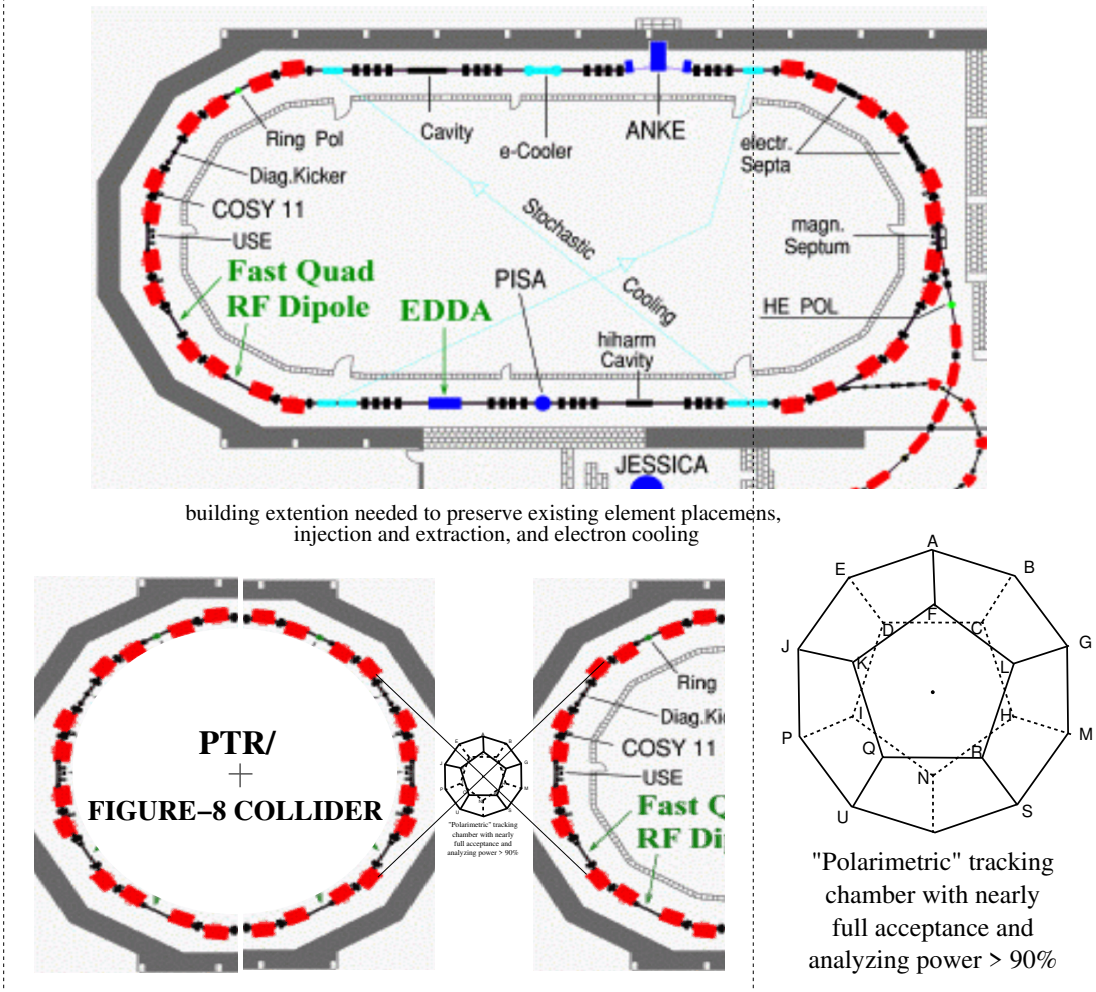

FIG. 5. This figure shows COSY-> PTR revision practicalities. East and west semi-rings powered, individually, almost, but not quite, fit into the COSY beam hall. Short of extending the building, there are numerous compromise solutions. By changing super-periodicity the components from one ring with 24 bends can be reconfigured as two 3/4 rings, each with 12 bends, with no change in the bend radius (but reduced maximum energy). No new bends nor quads would be needed. Magnet strength is not a serious issue, since the required beam energies are much less than current COSY capability. As shown installed in the COSY beam hall, the proposed figure-eight configuration sits more or less on the same footprint as for the dual, PTR ring (on the left) and the BA (beam accumulator) ring (on the right) . Unfortunately, the 90 degree crossover requirement increases the footprint length enough to exceed the COSY building length (with the right arc of COSY fixed). The increased space between the rings scarcely affects eventual conversion to PTR on the left, bunch accumulator BA on the right, as in the current PTR plan. This makes increasing the building length an attractive option. Or it may be possible to slide the figure-eight ring to the right, which could also be satisfactory.

peaking forward and back, makes the forward nuclear scattering amplitude immeasurable for charged particles. One cannot, therefore, consider using the optical theorem for *pp* scattering.

We note that the pseudo-scalar condition shown in Eq. (6), violates P-symmetry as well. As Lee and Wolfenstein[4] and Prentki and Veltman[5] explain, the most promising place to look for TVPC (T-violating, P-conserving) phenomena is in this region. Not included in the Standard Model, the TVPC coupling strength could be midway in strength between the weak and strong forces, of the same order as electric coupling, without having been detected at that time, nor still today. This is the basis for the name “semi-strong nuclear force”.

Following this advice, we therefore emphasize measuring cross sections for which the spin states are orthogonal to each other, and not parallel to either incident beam direction. Recognizing that contributions to the total cross section of terms like this may cancel on the average, we have to measure differential rates for all scattering directions.

Since the nearly forward/backward directions are made inaccessible by Rutherford scattering this cannot be perfectly achieved. However, in the fixed-target-laboratory-

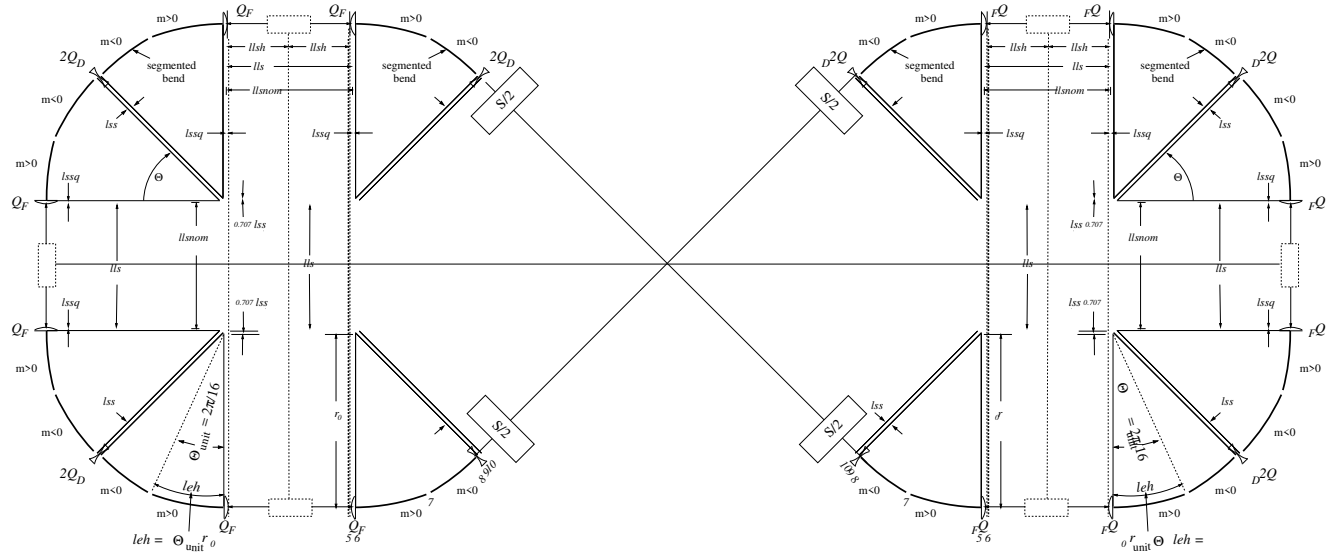

FIG. 6. This layout figure shows how a figure-eight all magnetic ring can be constructed from two partial rings, each identical to 3/4 of the PTR rounded-square ring described in the CERN Yellow report (CYR). The individual ring lattice design, copied from CYR, is by now outdated; but the figure is adequate for present purposes. With no electric bending the spin tune is $Q_s = 0$, ideal for low energy scattering measurement; but the EDM signal would not accumulate monotonically. Conversion of four sectors from magnetic to electric bending would produce measurable EDM response accumulation. Four boxes labeled "S/2" represent *half-snakes whose purpose is to cause EDM precession to accumulate monotonically (once some magnetic bends have been converted to electric such that the individual partial-ring spins are globally frozen), These snakes would be absent for the elastic scattering measurements described in this paper.*

frame equivalent energy range $150 < E < 400\,\mathrm{MeV}$, the scattering is known to be nearly isotropic, so the excluded forward and backward directions could either be ignored, or covered adequately using extrapolated phase-shift analysis.

In any case, since the optical theorem is not being used, minor limitation of angular coverage should be unimportant. This amounts to conceding that the proposed experiment fits into the sequential-measurement, category (i) in the formulation of Arash et al. This means that, to achieve a T-violation fractional upper limit of, say 10^{-3} or 10^{-4} will require a corresponding improvement in the relative normalization of forward and reversed-time rate normalizations. However, *by casting the experiment as a branching rate comparison, rather than as an absolute cross section comparison, our proposed scattering detection apparatus is designed to ameliorate this normalization challenge.* The following sections explain this approach.

3. TVPC contributions to *pp* and *dd* scattering

A paper by Yu.N. Uzikov and A.A. Temerbayev[31] investigates TVPC effects, saying, for example, "The observation of TVPC effects would be considered as indication of physics beyond the standard model". For our purposes it is the explicit isolation of TVPC terms (also referred to as "T-odd, P-even in their terminology) that is valuable. Copying from their paper, using standard formalism, the TVPC term, in a very general form, written in terms of Pauli matrices

$$\boldsymbol{\sigma} = \sigma_x \hat{\mathbf{x}} + \sigma_y \hat{\mathbf{y}} + \sigma_z \hat{\mathbf{z}}, \quad \text{is} \tag{7}$$

$$e'^{*}_{\beta} M(0)^{TVPC}_{\alpha\beta} e_\alpha = \tag{8}$$
$$\widetilde{g}\Big(\big(\boldsymbol{\sigma}\cdot(\mathbf{m}\times\mathbf{e})\big)(\mathbf{m}\cdot\mathbf{e}'^{*}) + \big(\boldsymbol{\sigma}\cdot(\mathbf{m}\times\mathbf{e}'^{*})\big)(\mathbf{m}\cdot\mathbf{e})\Big),$$

where $\widetilde{g}$ is the TVPC coupling amplitude, $\mathbf{e}$ and $\mathbf{e}'$ are polarization vectors of initial and final state protons, and $\mathbf{m}$ is the unit vector along the beam momentum (in our case $\hat{\mathbf{z}}$). Uzikov and Temerbayev also provide this amplitude in the compact form

$$M(0)^{TVPC}_{\alpha\beta} e_\alpha = \widetilde{g}\big(\sigma_i(\epsilon_{z\alpha i} m_\beta m_\alpha + \epsilon_{z\beta i} m_z m_\alpha)\big), \tag{9}$$

summed over index i, where $\epsilon_{\alpha\beta\gamma}$ is the usual fully antisymmetric tensor, $\sigma_i (i = x, y, z)$ are the Pauli matrices and the $m_\alpha (\alpha = x, y, z)$ are Cartesian coordinates of the vector $\mathbf{m}$[8]. This conjectured semi-strong amplitude needs to be summed along with the TCPC amplitudes,

A proposed strategy for detecting the presence of this amplitude, in order to determine $\widetilde{g}$, is to scan the initial spin states continuously and periodically through regions

[8] Note that, like Stodolsky, this paper defines $\mathbf{m}$ as unit vector directed along the incident beam in fixed target geometry.

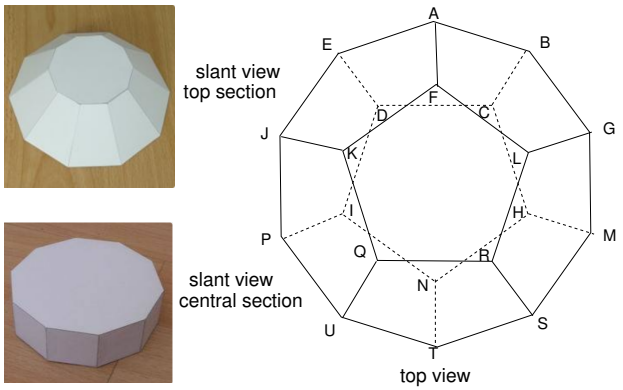

FIG. 7. Artist's conceptions of almost full-acceptance tracking/stopping/polarimeter chambers at a storage ring intersection point. The figure on the right is a true Platonic dodecahedron, with 12 identical planar faces, each subtending the same solid angle. Labeled vertices are for convenient reference in the text. For example, a "clean" stopping particle passing through the ABCDE face can be expected to be in coincidence with a clean stopping particle passing through the UQRST face. Despite appearances, vertices A,B,G,M ...E, in the idealized figure, do not actually all lie in a single plane. The figures shown on the left are somewhat more constructionally practical. Their planar and dodecahedral faces subtend roughly equal solid angles. To accommodate passage of the colliding beams there can probably be no useful particle detection in the central section.

for which this amplitude oscillates between maximally contrasting values.

The novel aspect of the proposed apparatus that makes this plan promising is the fact that the polarization states of one or the other scattered particle will have been measured for a significant fraction of the scatters. These distributions can be compared with known distributions of both conjectured foreground (i.e. TVPC) and known background (TCPC).

4. Previous *pp* tests of T-reversal symmetry

In pre-standard-model days, even before parity violation had been detected, there were experiments proposed and performed checking for T-violation. One important success was confirmation at the one percent level that scattering asymmetry P and analyzing power A are equal[9]. But small aperture scattering experiments have serious calibration difficulty. Experiments have involved as many as four sequential scatters. Eventually these experiments have contributed to precision parity violation investigations, but they have been too inaccurate for weak time reversal violation symmetry detection.

[9] Wolfenstein originally took this relationship to be obvious, but later confessed that he had overlooked the possibility of T-violation.

For example, Abashian and Hafner[32] obtained $A = 0.308 \pm 0.005$ and $P = 0.279 \pm 0.017$ for scattering asymmetry and analyzing power. This was confirmation of T-conservation of roughly 1 percent at the 2σ level. Davis et al.[33] measured $P - A = 0.0047$ at kinetic energy 198.5 MeV, with a statistical uncertainty of ± 0.0025 and a systematic uncertainty of ± 0.0015. Aprile et al.[34] found less than 1 percent T-violation at 579 MeV (well above pion threshold).

Of these $A-P$ tests (all consistent with T-conservation within error bars) the Davis et al. result, with A-P measured value treated as T-violation, provides the smallest upper limit ($|P - A| < 0.0084$ with 90% confidence), for elastic *pp* scattering below pion threshold. Enthusiasm for celebrating these symmetry-confirming "integrated" determinations needs to be tempered by the possibility that excessive scattering in one direction can be canceled by deficit in another direction. This could mask symmetry violating effects that might be visible on a finer-grained scale.

For qualitative discussion purposes in estimating how much improvement can be expected from new measurements, we will consider it likely that T-violating *pp* scatters in excess of one percent of all *pp* scatters would have already been recognized as such.

IV. LOW ENERGY ELASTIC *pp* SCATTERING CHARACTERISTICS

1. Total and differential cross sections

Historically, most *pp* and *dd* elastic scattering measurements have been made in a fixed-target laboratory frame. In this frame, physical considerations limit the region of interest to an energy[10] range from 150 to 400 MeV. Though below pion production threshold (at noticeable rates) at the high end, and energies at the low end large enough for nuclear scattering to be distinguishable from Rutherford scattering except in small forward and backward angular ranges. Furthermore these energies are known to be high enough for spin-dependent effects to be important.

(Curiously) it is also true, quoting Bethe and Morrison[35] that, throughout the range from 150 to 400 MeV, the *pp* CM elastic differential cross section is *constant* and given by

$$\frac{d\sigma}{d\Omega} = 3.4 \pm 0.4\,\mathrm{mb/sr}. \tag{10}$$

Notice that this implies that, as well being isotropic, the total elastic scattering cross section is independent of energy. As a consequence the total cross section is

$$\sigma = 3.4 \times 2\pi = 21.3\,\mathrm{mb}, \tag{11}$$

[10] "Energy" usually means "kinetic energy" while discussing low energy, elastic pp scattering.

(where multiplication by 4π solid angle would double count the scattering events.)

Fixed target nuclear scattering results obtained at COSY at energies above meson thresholds have been surveyed by C.Wilkin[16]. His paper includes important information concerning scattering and measurement capabilities at COSY.

2. Final state T-violation detection

Various T-violation searches are possible. A four bunch configuration with all particles in each single bunch in the same pure spin state, but bunch polarizations individually controlled, bunch by bunch, has been illustrated in Fig. 4.

Only conventional counting rate methods have been discussed up to this point. There are also methods made possible by historically published polarization data. Based on existing data, in spite of the fact that the scattering is more or less isotropic, the spin-flip rates in *pp* scattering are known to be appreciable, and to depend on polar and azimuthal scattering angles. For the small aperture Davis et al. differential scattering data point (at 16.5° laboratory scattering angle) the spin-flip fraction was $S \approx 0.40$.

A T-violation easy to visualize for an individual scatter, would be for one spin to flip while the other does not. The proposed scattering detection apparatus is sensitive to this amplitude because the incident spin states are known and the scattered state polarizations are measured.

The discussion leading up to Eq. (6) suggests that T-violation is most likely when spin vectors $\mathbf{s_p}$ and $\mathbf{s_d}$ are more or less orthogonal to each other, with neither parallel to either beam direction. As a consequence, violation of T or P symmetry is expected to favor conditions for which $\mathbf{s_p} \times \mathbf{s_d}$ is maximal.

Separating T and P violation[11] would require distinguishing a $(\mathbf{s_p} \times \mathbf{s_d}) \cdot \mathbf{m})$ distribution from the distribution proportional to

$$\big(\boldsymbol{\sigma} \cdot (\mathbf{m} \times \mathbf{e})\big)(\mathbf{m} \cdot \mathbf{e}'^{*}) + \big(\boldsymbol{\sigma} \cdot (\mathbf{m} \times \mathbf{e}'^{*})\big)(\mathbf{m} \cdot \mathbf{e}) \qquad (12)$$

(where $\mathbf{e}$ and $\mathbf{e}'$ are to be replaced by $\mathbf{s_p}$ and $\mathbf{s_d}$ in either order) as given by Eq. (8). Maximizing $\mathbf{s_p} \times \mathbf{s_d} \cdot \mathbf{m}$ requires the three vectors to be mutually orthogonal. As it happens, in this case the terms of Eq. (12) vanish individually. This suggests a kind of "lose or win-win" outcome from the experiment. Symmetry violation *undetected*, is a loss. If symmetry violation *is detected* (a win) then it should be possible to isolate T-violation and P-violation components; (another win).

[11] The possibility of separating T and P violation in the present context may be academic. As stated previously, with TPC-conservation guaranteed, and C-conservation not at all implicated, T- and P- violations must be correlated such that TP is conserved.

3. Spin configurations

Based on accelerator physics considerations, for the beam polarization to survive indefinitely requires the bunch polarizations to be predominantly "up" (i.e. pointing vertically up) or predominantly "down". For best polarization survival this alignment would be perfect, but previous discussion has argued that no T-violation would then be likely—non-zero triple product "volume" is essential.

The plan, therefore, has to be to superimpose significant horizontal polarization components on predominantly vertical bunch polarizations, for example as shown in Fig. 4. The incident protons can be assigned mutually orthogonal transverse spin components which result in (local-) precession of both incident proton spins around the vertical axis consistent with (global) spin tune $Q_s = 0$, so that the cross product $\mathbf{s_2} \times \mathbf{s_4}$ remains parallel to the vertical axis. Geometrically, the "volume" defined by the triple product $(\mathbf{s_2} \times \mathbf{s_4}) \cdot \hat{\mathbf{z}}$ (a pseudo-scalar) then remains constant.

With a figure-eight lattice shape the global spin tune vanishes, but the polarized beam bunches are only pseudo-frozen. Precession accumulation in one "arm" of the figure-8 unwinds in the other. There is no need to stabilize this motion. It happens automatically. Yet the ψ angles of the separate beam bunches can be initialized individually (by some fraction of 2π) during beam preparation. At any particular point, for example at the IP collision point, the spin state is frozen.

The polarization vectors of colliding bunches **b2** and **b4**, though not necessarily the same, stay constant in time, individually. Beam preparation with individual bunch polarizations controlled independently (using pulsed transmission line Wien filter) has been demonstrated at COSY[21].

Though the orientations of polarization vectors **s2** and **s4** at the IP, are constant on a fast (beam revolution) time scale, their relative orientation can be changed adiabatically on a long time scale measured, say, in seconds. Gradual alteration of the relative orientations of **s2** and **s4** is unlikely to be noticeable for PCTC scatters, but may be noticeable for PVTV (P-violating or T-violating) scatters, especially for relative orientations of **s2** and **s4** that have been chosen to enhance PVTV scattering amplitudes.

During this precession the T-violation "forbiddenness" may oscillate sinusoidally between excluded and favored regions defined by the TVPC amplitude Assuming there are two circulating bunches in each beam, with one spin up and one down, the scattering amplitudes would acquire per bunch factors

$$F_1 = \cos\phi, \quad \text{or} \quad F_2 = -\cos\phi, \qquad (13)$$

where ϕ is a cylindrical coordinate angle. Data collection can continue for full run durations, with ϕ varying adiabatically.

4. Detection chamber polarimeter properties

Referring back to the Arash et al. categorization into experiment types, this proposed experimental configuration might seem to fit into the type (ii) "self-conjugate" type—forward-time and reversed-time reactions being measured with identical apparatus. This is not precisely the case, however. The beam currents of bunch 1 and bunch 2 will not be exactly equal, and their spin directions reverse under time reversal. Neither will the apparatus be exactly left-right nor exactly up-down mirror symmetric.

Formally, the experimental apparatus is of category (i)—it is not exactly self-conjugate. But the apparatus is very nearly symmetric in most ways and there are beam-based procedures that can greatly reduce normalization systematic uncertainties to well below levels values that Arash et al. suggest may be irreducible. Furthermore, with nearly full solid angle aperture coverage, rate determinations become branching ratio determinations rather than cross section measurements. Whereas the "denominator" in a small aperture cross section measurement is a hard-to-determine solid angle, our branching ratio normalizing factor is a fixed total number of "good" events. Small solid angle apertures and near 4π solid angle denominators are subject to systematic error, but the fractional error is much less in the near 4π case.

Furthermore, expressed as a branching ratio case, the same denominator will be common to the two rates being compared. Though the experiment is of category (i) in the Arash labeling, the normalization uncertainty can become small relative to counting statistic errors.

It is known, from Iberaku et al.[36] that, in the range from 40 MeV to 80 Mev, integrated elastic and inelastic p-carbon scattering cross sections are approximately equal. See also Fig. 12.

The tracking chamber foil thicknesses must be thin enough that no particles "range out undetected" even at the lowest particle energy. Best foil thickness compromises have been worked out, especially, by Ieira et al.[37]. (A very small set of) their measured analyzing powers for scattered proton polarimetry are shown in Fig. 8.

These graphs are applicable to graphite which may be impractical as plate material for a tracking chamber. Perhaps multiplane graphene or graphite foil such as used by Ieira[37] could be used. Otherwise the graphite plates might have to be sandwiched between thin conducting foil, such as aluminum which, itself, provides significant polarization analyzing power. The polarimetric properties of low-Z materials do not depend strongly on Z[38].

From existing measurements and models, with both initial spin states being known with near certainty, the left/right and up/down asymmetries of every scattered proton can be predicted with quite good accuracy. Based on the one million primary scatters for which at least one p-carbon scatter is observed, the dominant statistical uncertainty in dual-detected scatters will come from fluctuations in the p-carbon scatter of the other proton.

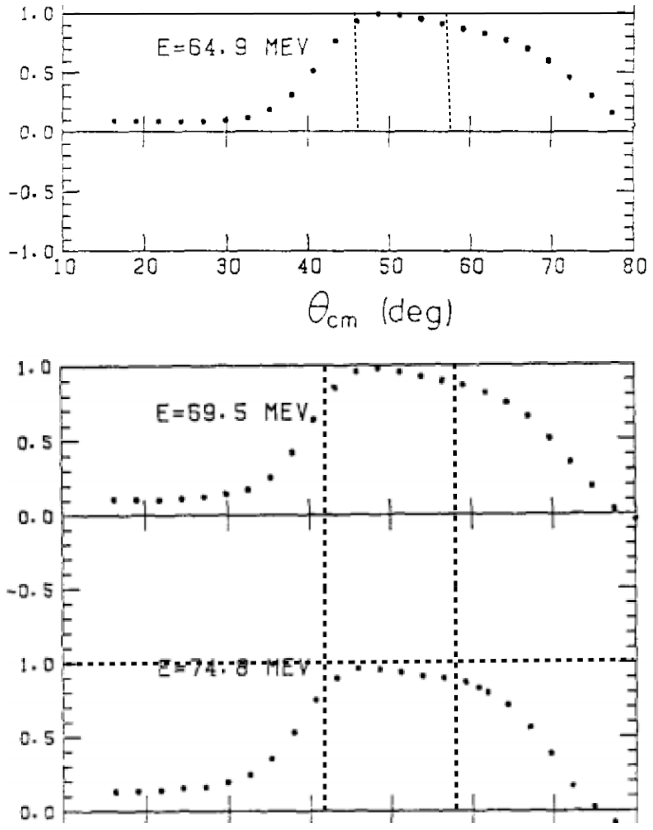

FIG. 8. Analyzing powers for left/right carbon-scattering proton polarimetry[37]. At all energies shown the analyzing power peaks above 0.99 and remains higher than 0.9 in the angular range from (for example) 45 to 60 degrees, where it can be accurately approximated by a polynomial fit tangent to the point at which the efficiency is 100 percent. With angular bins of one percent width in analyzing power, regions of predictably-high probability spin-flip violation can be accurately delineated. Extended from 100° to 170°, the plots are mirror symmetric about $\pi/2$. Since the angular distribution is known to be quite accurately isotropic, this high sensitivity region represents roughly 1/4 of all events. Of these an elastic scatter occurs with high probability in the first 1/4 of the proton stopping range. Especially valuable will be the one in 400 fraction of single scatters for which the polarizations of both scattered particle are measured with high analyzing power.

V. UNBALANCED SPIN-FLIP T-VIOLATION DETECTION

1. Coarse integrated polarimetry averaging

There is a clear statistical advantage for triplet incident states in which particle spins in both beams are all "up" or all "down". In this case, there could be an overwhelming preservation of the same overload in the scattered states. This would improve the selectivity for detecting scatters with unmatched spin flips.

But these are states for which T-violation is probably unlikely. Previous discussion has suggested that T-

violation (or P-violation) detectability favors spin configurations for which triple products formed from the spin vectors of incident or scattered particles, along with any momentum vector, do not vanish. For long spin coherence time (SCT) one favors incident conditions with predominant "up" (or "down") polarization for both incident bunches. To maximize T-violation sensitivity this vertical component is best augmented by mutually orthogonal transverse polarization components, as shown, for example, in Fig. 4. [12]

The "analyzing power" A in left/right scattering asymmetry for N scattered particles is defined by

$$A = \frac{R-L}{R+L} = \frac{R-L}{N}, \tag{14}$$

where R, L, and $N = R + L$ are, respectively, the numbers of right, left, and total scatters. Though R and L are stochastic quantities, subject to counting statistic uncertainty, it is usually legitimate to treat N as the unambiguous total number of scatters. In this case it is a branching ratio, rather than an absolute cross section, that is being determined. It is then natural to introduce normalized "branching ratios" satisfying the relations

$$p = n_R = R/N; \quad q = n_L = L/N; p + q = 1, \tag{15}$$

where p is the right-scatter probability and q is the left-scatter probability. Substitution of these equations into Eq. (14) produces

$$p = \frac{1+A}{2}; \quad q = \frac{1-A}{2}. \tag{16}$$

On the other hand, the "efficiency", E, in scattering asymmetry covers the common situation in which R and L are normalized by a number $N_{\rm incident}$ which is the total number of particles passing thought the polarimeter, most of which register neither in the right nor the left detector. Then one defines efficiency E as the fraction of incident particles that actually register in the polarimeter;

$$E = \frac{N}{N_{\rm incident}}. \tag{17}$$

In this case it is appropriate to treat N as stochastic.

Usually, in polarization measurement, there has to be a trade-off made between high efficiency, mediocre analyzing power, and low efficiency, high analyzing power. What has typically been used in historic pp polarization measurements can be characterized as low efficiency, $E < 0.0001$, and fair analyzing power, $A_{\rm min} \approx 0.4$. Along with the high efficiency $E \approx 1/400$ (the probability that an 80 MeV proton stopping in carbon will suffer an elastic nuclear scatter) the main design concept for the present proposal is to concentrate on detection of scatters for which polarimeter analyzing powers are as close as possible to 100%. In any case, best T-violation selectivity will require strong weighting of data from high analyzing power regions.

Selective detection of T-violating scatters depends critically on the analyzing power of the polarimetry, which is, itself, dependent on scattered proton energy. For best selectivity it is appropriate to weight most heavily data in regions for which the analyzing power is highest. For simplicity, so far, no such weighting has been established. Rather, a quite low "average" analyzing power $A = 0.4$ has been assumed. Mathematical analysis with mediocre analyzing power is given in connection with Fig. 9.

2. Anticipated data rates

Anticipated data rate performance can start with the calculated storage ring luminosity of 10 inverse millibarns per second, capable of producing $N_0 = 2 \times 10^9$ clean scatters per year, as calculated in Appendix C. Of these events, a number $N_1 = 10^7$ will provide p-carbon polarimetry for one or other of the final state protons, including $N_2 = 25,000$ for which both final state proton spins have been measured; with a fairly small fraction of these referred to as "gold-plated", these events are "silver-plated". All these rates are tabulated in Table IV.

Note, however, that in a certain sense, modulo polarimetric inefficiency, the kinematics, including spin, of every one of the $N_1 = 10^7$ single polarimetric-detected events have been fully-determined. This assumes time-reversal symmetry, along with the concession that time-reversal violation will occur only at the one percent level. One hopes this fraction will exceed one percent but cannot expect this to reduce the sample size appreciably. From these data rates it is not obvious which class of events holds the best statistical power for detecting T-violation.

event class	symbol	formula	fraction	symbol	events/year
pp scatter	N_0	1	1	N	2×10^9
single spin meas.	N_1	$2/E$	$2/400$	N_1	1×10^7
double spin meas.	N_2	$2/E^2$	$2/400^2$	N_2	0.25×10^5

TABLE IV. Anticipated event rates with increasing detection quality per nominal year running time for polarimetric detection efficiency $E = 1/400$.

Let us consider the experimental problem of detecting a correlation between initial and final spin coordinates, on the one hand, and scattering directions on the other. Based on many historic experiments, experimentally measured cross sections have been parameterized to

[12] It is experimentally challenging to maintain beam polarization at fixed polar angle relative to "up" or "down". This requirement is similar to optimal conditions for EDM measurement, for which the spin remains horizontal, always pointing approximately forward or backward, with polar angle equal to $\pi/2$). Such beam polarization stability has been successfully achieved in COSY.[23]

best fit, PCTC (P and T-conserving) theoretical production models. These distributions have been and can now be digitally reproduced with high accuracy by Monte-Carlo simulation, as parameterized by best fit partial wave expansion coefficients.

One now speculates that, hidden in this data, is a PCTV, time-reversal violating contribution with differential cross section at perhaps the one percent level, which has so far evaded detection. We propose, therefore, to study the same process by direct measurement. This might be called "analog Monte-Carlo determination". The reason we have to acknowledge the stochastic nature of the measurement, is that we have only beams with less than 100% polarization and polarimetry with less than 100 percent analyzing power.

A requirement of T-symmetry is that, if one spin flips, so also does the other. The PCTC (P-conserving, T-conserving) fit presumably satisfies a constraint $N_u = N_{\rm null}$ where $N_{\rm null}$ is the (dominant) theoretical rate, calculated from already-known "measured cross sections" with no apparatus equipment prejudice concerning the fractional contribution of T-violating or P-violating processes, but the theoretical expectation that these contributions have been smaller than some small value, such as one percent.

In our proposed experiment, frozen-spin monochromatic protons in independently adjustable (almost) pure spin states collide inside a nearly 4π acceptance polarimeter. The CM system motion in the lab is modest and scattered energies are identical. Both scattered particles will stop in nearly full-acceptance tracking chambers. Some will undergo nuclear scatters in the tracking chamber plates. This will provides polarimetry, for example with efficiency $E \approx 1/400$ and analyzing power $A \approx 0.96$.

At the cost of some duplication, to reduce confusion between scattering statistics and polarimetry statistics, one can switch variables in formulas (17) through (17) from R and L to N_u and N_d, which are the (unknown) numbers of "up" and "down" protons in a scattered beam. In the proposed experiment this amounts to treating pp scattering as "virtual polarimetry" for which the "up" or "down" state of each scattered proton has not yet been detected.

For convenient reference to conventional statistics notation we will, however, retain p and q, satisfying $p+q = 1$, as the probabilities of events satisfying the binomial distribution. And, for numerical example in the proposed experiment, the typical numerical values of analyzing power and efficiency are very different from conventional polarimetry.

For example, we use the value $A = 0.96$, which produces $p = n_u = N_u/N = 0.98$ and $q = n_d = N_d/N = 0.02$ with p and q fractional (i.e. summing to 1) binomial distribution probabilities. As a binomial distribution, standard deviation about the mean (the same for both N_u and N_d) is given by

$$\sigma_{\rm binomial} = \sqrt{Npq} \stackrel{e.g.}{=} 0.14\, N^{1/2}. \tag{18}$$

Quoted with error bars, relative to the null-expected rate, according to this standard deviation, the measured up-rate will be

$$N_u = pN_{\rm null}\Big(1 \pm \sqrt{\frac{pq}{N}}\Big) \stackrel{e.g.}{=} \mathbf{N_{u,measured}}\Big(1 \pm \frac{0.14}{N^{1/2}}\Big), \tag{19}$$

where (with $\mathbf{N_{u,measured}}$ shown bold-face for emphasis) the statistical significance of deviation from a null distribution mean can be quantified by its magnitude in units of the "±error" term. The merit of this formulation in the present context is that the error can be calculated without the need for having actual data.

For the sake of definiteness, let us tentatively presume a current upper limit T-violating contribution of $\widehat{\sigma}^{\rm current\ T-ViolFrac} = 0.01$ exists, with error bars $\pm\sigma_{meas.} = \pm 0.01$. This would match the supposition that any higher fraction would have already been detected. The experimental challenge will be to produce a T-violation signal with systematic error smaller than the counting statistics error.

Distinguishable particle scattering (such as pd) would be more easily interpretable than our pp case, in that a proton appearing in one chamber would always be accompanied by a deuteron in the opposite chamber. Nevertheless, since Eq. (19) represents the uncertainty in what has actually been measured, we substitute $N = 5 \times 10^6$ into Eq. (19) to produce an estimated fractional statistical error

$$\begin{aligned} \sigma_{est.} = \frac{0.14}{2236} &= 0.63 \times 10^{-4}, \text{or} \\ \text{T-ViolFrac} &= 0.01 \pm 0.63 \times 10^{-4}. \end{aligned} \tag{20}$$

Preliminary and vague as it is, this evaluation is given only to suggest that T-violation at significantly low levels should be achievable. Averaged over all directions, this fractional error is likely to be misleading since the measured polarizations themselves may tend to cancel on average. More granular estimations, based on judicious preparation of the incident bunch polarizations, follow.

3. Two particle T-violation detection

The binomial distribution, for N_2 trials, of "success" with probability p and "failure" with probability q is

$$P(x) = \frac{N_2!}{(N_2 - x)!x!}\, p^x q^{N_2 - x}. \tag{21}$$

This function is plotted in Fig. 9 for $p = 0.58$, $q = 0.42$, and $N_2 = 10$, 100, and 1000. These plots show the distribution of outcomes identified as "successes". Failure distributions, also summing to 1, are not shown—they would have the same shapes, but centered on 4.2, 42, and 420.

It is instructive for understanding the logic, to start by calculating the probability of correct determination

for a single particle spin flip using a polarimeter with the mediocre, $p = 0.58$, $q = 0.42$, probabilities exhibited in these graphs. Already with 10 events, the average success probability exceeds 1/2. For data sets with N_2 increasing beyond 10, the success probability approaches $p = 0.58$ and the failure probability approaches $q = 0.42$.

Supposing (without justification) that protons from a 100% "up"-polarized beam produce only "up"-polarized scatters, consider a scattered proton entering a polarimeter for which $p = 0.58$ represents the probability of its spin state being properly identified. Supposing T-violation consisted only of events with one spin flipping and one not, p and q could be described as "null probabilities" in the sense that, with no T-violation, the true distribution has no spin flips. In the large sample limit a collected data set would then be expected to center on $x = 0.58$, because this is the fraction of correctly identified polarizations.

Contemplating the presence of some T-violating scatters, we would interpret deviation of the peak position from x=0.58 as indication of T-violation. Regrettably, we do not actually " understand the probabilities". The true analyzing power power will not, in fact, be constant, independent of kinematic parameters, nor will it even be exactly equal to $A = 0.4$ "on the average". Though ameliorated by calibration efforts, this will inevitably leave detection of T-violation, purely on the basis of deviation from a calculated value (such as 0.58) as dubious.

In conventional language, for small samples, the uncertainty will be dominated by statistical uncertainty but, for large samples, the uncertainty will be dominated by systematic errors resulting from our imperfect understanding of the apparatus.

To reduce this systematic error it is important for the polarimeter analyzing power to be as high as possible—at 100% there would be no systematic error. In the proposed experiment, a quite small fraction of the detected scatters will have analyzing power greater than 0.99, but a substantial fraction will have a, still respectable, analyzing power greater than 0.9.

In an experiment intending to test T-conservation the distinguishing signal for T-violation is that, if one spin flips, so also must the other. If spin-flips were forbidden by T-conservation (*which they are* n*ot*) then any detected spin-flip would provide evidence for T-violation. To reduce confusion it is sensible for initial spin states to be set up to be the same, say "up". Then any detected "down" polarized scattered proton would provide evidence of T-violation. Since *some T-conserving amplitudes* do *involve spin-flips*, the true situation would be much more complicated, except for the fact that, for T-conservation in elastic scattering if one spin flips, so must the other. T-conserving scatters must "match" in this sense.

As a consequence, except for different interpretations and values for the p and q probabilities, the T-violation probabilities associated with correctly identifying T-violation using "mismatched" spin flips is described by

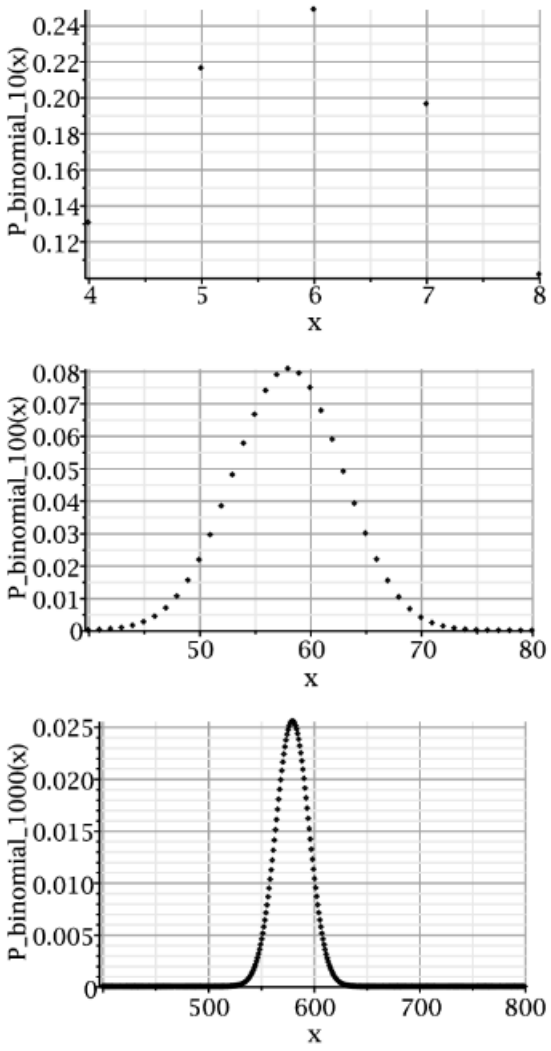

FIG. 9. Binomial probability functions with $p = 0.58$, $q = 0.42$, for $N_2 = 10$, 100, and 1000 samples. Irrespective of the value of p and $q = 1 - p$, the probabilities of correct and incorrect T-violation identification sum to 1. Failure distributions are not shown—they would have the same shapes, but centered on 4.2, 42, and 420.

the binomial distribution, Eq. (21), as for the single particle T-violation described previously. (This is why the number of events was expressed there as N_2.)

The least ambiguous signature for T-violation is one spin flipping, and one not. Actually, both identifications being wrong provides information equivalent to both being correct, as far as T-violation detection is concerned. As a result, in our 98% analyzing power set-up, the two particle correct T-violation identification probability is: $0.98 \times 0.98 + 0.02 \times 0.02 = 0.9608$. The probability of one correct and one incorrect identification is $2 \times 0.02 \times 0.98 = 0.0392$. Conservation of probability, confirmed by doing the arithmetic, is reassuring.

Let us assume $N_1 = 5 \times 10^6$ events, for which all kinematic parameters are known and at least one scattered

particle's polarization, have been recorded. For each event there is also a recorded "phase angle" ψ providing the instantaneous orientations of both input spin vectors in spin-space. For now this is just a tallying mechanism for associating the instantaneous polarization measurement with the other particle parameters in effect when the polarization measurement was made. Each of the measured polarization values can then be compared with the previously established "null polarization values".

Of the events just discussed, about $N_2 \approx 0.25 \times 10^5$ events, will contain spin information about both scattered particles. Some, with almost 100 percent analyzing power, were referred to earlier as "gold-plated". Even a few events in which one spin flipped, and one did not, would prove the existence of T-violation. Further statistical analysis of these events is far too difficult to be attempted in the present paper.

VI. "SPIN TRANSPARENCY" APPLICATIONS

1. History

The concept of "spin transparency", was introduced and defined in 2016 by Derbenev [39]: "In a figure-8 collider, the spin first rotates about the vertical field in one arc. This rotation is then undone by the opposite field in the other arc. The resulting effect of the strong arc dipoles on the spin dynamics reduces to zero over one particle turn and the whole ring becomes transparent for the spin." The concept is more fully developed and explained in Filatov et al. [40]

"Spin filtering", a term introduced before 1968 and still in use, is explained in reference [41]:"As long ago as 1968 it was realized that by means of a "spin filter" using an internal polarized hydrogen target polarized high-energy proton beams could be produced at the 30 GeV intersecting storage ring (ISR) at CERN." Superficially at odds with spin transparency, spin filtering emphasizes scattering *dependence on*, not *independence of*, spin state.

The spin-filtering method exploits the spin dependence of the total *pp* cross section[16]. For beam and target polarized transversely in the y-direction, the proton-proton total cross section has the spin structure

$$\sigma_{\rm tot} = \sigma_0 \pm \sigma_1 \cdot PQ \tag{22}$$

Where σ_0 is the spin-independent part, σ_0 the spin-dependent part. P is the beam polarization and Q that of the target. Thus, if σ_1 is non-zero, the *pp* total cross section will depend on the relative orientations of the beam and target spin orientations. The positive (negative) signs denote a parallel (anti-parallel) orientation of the spins of beam and target.

In the context of the present paper, it is "spin transparency" that contributes to nuclear spin physics by providing the accelerator physics capability to study T-violation in low energy nuclear physics—for both elastic scattering and deuteron EDM measurement.

A property that makes the term "transparency" apt, is that, regarded as an approximate method, the transparency approximation can be most valid, usually on long (adiabatic approximation) time scales, or, more surprisingly, on short (sudden approximation) time scales. The next subsection shows how adiabatic sinusoidal variation of beam spin states can provide Fourier sensitivity enhancement to enable experimental detection of T-violation in *pp* scattering. An example of application of spin transparency on a fast time scale is given in the subsequent "Recovery of deuteron EDM sensitivity" subsection.

2. Adiabatic sinusoidal variation of spin states

1. Fourier sensitivity enhancement

"Can One Hear the Shape of a Drum?" is the title of a 1966 article by Mark Kac in the American Mathematical Monthly which made this question famous. Not having read the article (since the title expresses a question rather than an answer) one can ask a similar question in the present context: "With the proton assumed to be composite, rather than elementary, can internal proton variability have a measurable effect on "elastic" *pp* scattering?".

A routine procedure of experimental mechanical engineering is to scan in frequency a harmlessly small sinusoidal signal applied more or less arbitrarily to a physical structure, in order to determine frequencies at which strong drive might be harmful. Applying the principle that any linear response must have the same frequency as the drive, synchronous detection can make such such procedures extremely sensitive.

Here, for elastic proton scattering, we conjecture that the answer to this question is "yes". A collision between two protons could temporarily stir up the contents of the proton enough to affect the elastic angular scattering distribution while producing no other detectable particles nor any measurably-large loss of proton energy.

The angle ψ was introduced in Fig. 4 with both of the considerations just introduced in mind. A way suggested to enhance the statistical sensitivity to T-violation is to vary ψ sinusoidally and detect the polarimetric response synchronously.

The Fourier series capability is especially valuable for statistically "noisy" data. In our case the statistical power of individual events varies over such a large range that most of the events provide little help in studying spin dependence. Yet It is hard to devise a bias-free strategy for filtering promising events from useless events. With relatively few significant Fourier coefficients being expected, for example three, constant term plus fundamental harmonics, it is useful to allow every event to contribute to every coefficient, with the expectation that the contributions from especially noisy events will cancel on the average.

This Fourier series capability should be especially useful for analyzing the $N_1 = 5 \times 10^6$ "silver-plated" events for which the spin of just one final state proton has been measured.

2. *Refined T-violation identification*

The data analysis prescription described initially, had nearly full aperture capture and high efficiency, but with only fair polarimeter average analyzing power of about 0.4 can be characterized as somewhat discouraging. With 100 percent analyzing power this would not be the case but, with weak analyzing power, the polarimetry data may not be able to demonstrate T-violation superimposed on a T-conserving distribution with high confidence. The most effective way to improve the situation is to improve the analyzing power. This consideration has led to the proposed figure-eight lattice operating just above the 69.5 MeV energy at which the analyzing power is as close to 1 as possible.

Furthermore, the ability to prepare the initial spin states optimally permits tailoring conditions to improve the T-violation selectivity. We proceed to analyze the probabilities associated with data sets defined for the proposed figure-eight lattice. By judicious steering of the initial state spin amplitudes one can alter the data collection procedure to "enhance the detectability" of T-violation.

What one is seeking, as evidence of T-violation, is the detection of correlation between spin coordinates and momentum coordinates. Measurements sensitive to such correlation have only been hinted at so far, in the form of defined data set records and results. One wishes to program a sequence of initial spin states at which elastic scattering is to be measured. One could, for example, pick a most promising initial spin state configuration and run for a year, changing nothing. Another extreme would uniformly scan the four dimensional spin space of incident polarization orientations. Neither of these approaches seems advisable.

A sound plan is to define a 1D closed path in spin space to be followed by continuously changing one or both of the *initial state* beam polarizations. On any such path, from extensive historical measurements, one knows, "null" expected *final state* distributions. One such scanning pattern has been illustrated in Fig. 4.

Possible final state amplitudes, intentionally neglected in existing experimental fits, such as TVPC, TCVP, and so on, have been mentioned in previous sections of this paper. And arguments have been given for the advisability of taking a data collection path that systematically alternates between violation-favored and violation-disfavored regions of spin-space. Though limiting the set of sensible paths, these considerations do not determine any particular "most promising" path.

A superficial discussion has been give in Section III 4 concerning kinematic conditions in which TCPC, TVPC, TCPV, TVPV scatters are known theoretically to be subject to the existence or non-existence of T-violation and/or P-violation scattering amplitudes. Such investigations have been performed in the past, but none with the presently proposed, (nearly) complete outgoing particle acceptance and high analyzing power polarimetry. Such a theoretical analysis has not yet been begun, let alone finished. The presumed outcome would be to have identified a favorable closed path in spin-space with non-vanishing T-violation amplitudes or, possibly, alternating between T-violation-favored and P-violation-excluded regions.

As mentioned earlier, in the kinematic region of the proposed experiment, the measured differential scattering cross sections are quite accurately isotropic, in spite of being the superposition of a complicated array of (numerous, but well-known) partial wave amplitudes, most of which are far from isotropic. (Curious in itself) this must mean that the superficial isotropy follows from the summing and averaging over spin states. In the proposed experiment (except for interchange of scattered particles to account for their being identical particles) no summing nor averaging of amplitudes is to be performed. One anticipates, therefore, that the single and double polarizations will differ significantly as functions of scattering directions.

Because known partial wave amplitudes have been constrained to be consistent with T- and P-conservation imposed constraints, to the extent there actually *is* a T-violating cross section, the "known" partial wave amplitudes are not actually correct. In the spirit of perturbation theory we begin by neglecting this defect.

Nevertheless, the data sets will be periodic functions of the ψ-phase angles. With the data represented as a periodic function, with period 2π, it is natural to convert the data sets into Fourier series. The proton beam polarization could advance nominally (for example) as

$$\mathbf{s_p} = \cos\psi\,\hat{\mathbf{x}} + \sin\psi\,\hat{\mathbf{y}}. \tag{23}$$

but with individual bunch phases separately adjusted. The T-violation evidence will then be contained primarily in the constant term plus the lowest harmonic sine and cosine coefficients of the Fourier series expansions of the data sets.

The uncertainties in these T-violation determinations should be dominated by statistical errors. The systematic error should also be quite small, since the data will be "self-normalizing"; the normalization will be established by the constant term of the Fourier series. Presuming that the double-polarization data is more statistically significant, the single particle measured polarization data, should provide a self-consistency check.

One can next consider restricting the analysis to regions for which the polarimetry analyzing power is well above average. A significant fraction of *pp* scatters will have laboratory scattering angles (which are also symmetric laboratory angles, in the angular ranges from 40° to 57°, shown bounded by broken lines in Fig. 8. In this

range (and in the same opposite-hemisphere range) the polarimetry analyzing power starts above 97%. Furthermore, mentally-interpolating from the upper and lower plots in Fig. 8, the analyzing power will exceed 70% for something like one-half of their full-ranges in the tracking chamber.

Some relevant trigonometric values are $\cos 0 = 1.0$, $\cos 40 = 0.766$, $\cos 57 = 0.545$,$\cos 90 = 0$. With the angular distribution uniform in $\cos\theta$, the fraction of solid angle bounded by broken lines in Fig. 8 will be $0.766 - 0.545 = 0.22$. This fraction, roughly 1/5 of all elastic scatters, possess "super-initial-analyzing power" polarimetry.

3. Recovery of deuteron EDM sensitivity

Of the low mass atomic nuclei, because of its small anomalous moment, the deuteron is the closest to being an ideal "Dirac particle" in that its spin is most nearly frozen in a pure magnetic field. One consequence, as noted by Yuri Senichev [42], is that deuterons can be frozen in a predominantly magnetic field, such as the figure-8 ring under discussion, with sectors alternating between positive magnetic and negative bending sectors. See Figure 10.

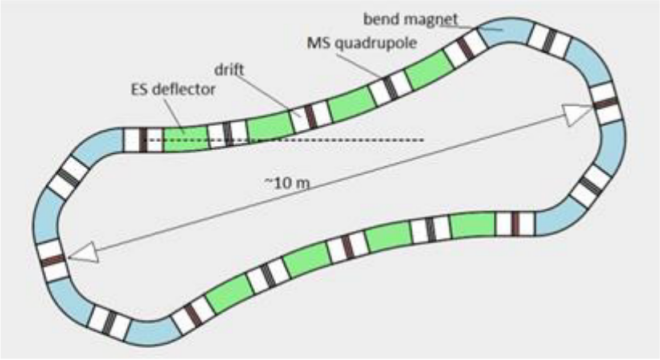

Figure 2: Ring lattice based on QFS concept.

FIG. 10. Screen-dump (including original figure caption) from reference [42], this figure shows the lattice proposed by Yu. Senichev for freezing deuteron spins with electric bending small compared to magnetic, to measure the deuteron EDM. In the present paper a similar capability is described in Section VI 3

.

Near the top of Figure 3 it is noted that there in no monotonically accumulating EDM signal. The reason for this is that there is only magnetic bending, in spite of the fact that the spin tune Q_s vanishes. The caption to Figure 6 notes the presence of boxes labeled S/2 in the figure, stating that they represent half-snakes that are turned off during *pp* scattering measurement, also also that they represent *half-snakes whose purpose is to cause*

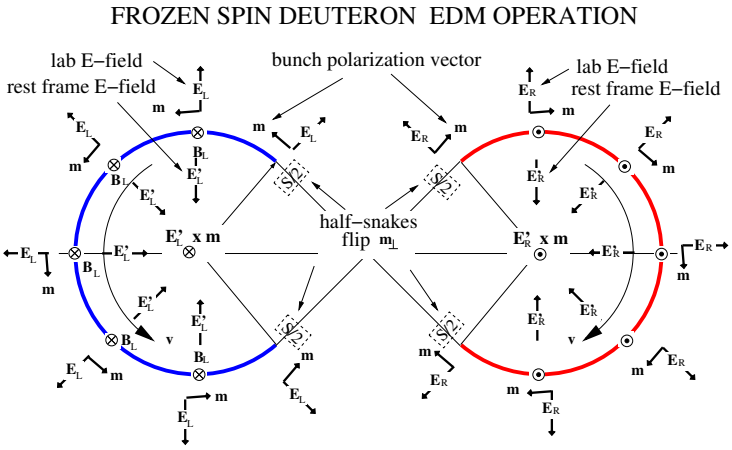

FIG. 11. Lab and CM electric and (dominant) magnetic fields are shown for figure-8 deuteron EDM measurement. A longitudinally polarized deuteron beam circulates as indicated by the curved velocity arrows. Curiously, the superimposed electrical bending is centrifugal and weak, but the magnetic bending is dominant and centripetal, as in the Senichev design. As given in Table III the bending fractions for frozen spin are $\eta_E = -0.17243$, $\eta_M = 1.17243$. In the rest frame, where the magnetic force is zero, the electric fields, Shown as E'_L or E'_F are centripetal, as required for circular motion. Furthermore they cause the beam to be globally frozen, at least, for example, in the right arc. But, with magnetic bending opposite in left and right arcs, the orbit is circular, with spins frozen in both arcs. The spin tune then vanishes, $Q_s = 0$, as required by figure-8 geometry. In this configuration any out-of-plane, EDM-induced precession produced in the right arc is canceled in the left arc. As a consequence, any EDM-induced precession caused in one arc would be canceled in the other (as indicated by the cross products shown at the center of each circle). The purpose for the paired solenoidal half-snakes in the cross-over lines is to overcome this problem. With the nominal beam polarization longitudinal, the orientation the MDM vector is aligned with the solenoid axis and the snakes effect neither the closed orbit nor the spin orientation. However, the effect of each pair of half-snakes is to reverse any EDM-induced out-of-plane beam polarization (indicated by $m_\perp$ in the figure; $\mathbf{m}_\perp \to \mathbf{m}_\perp$, which produces the desired monotonically accumulating EDM sensitivity.

EDM precession to accumulate monotonically (once some magnetic bends have been converted to electric such that the individual partial-ring spins are globally frozen).

Later, at the end of Section VII, it is stated that "For EDM measurement two solenoid Siberian half-snakes would be required in the beam crossover lines, to preserve already-established out-of-plane EDM-induced procession. However, the separate partial rings must also have separately vanishing spin tune. Otherwise, transverse polarization errors entering the crossover region would be reversed by the Siberian snakes, only to be further amplified by the subsequent opposite sign bending. This condition would therefore need to be feedback stabilized."

VII. PTR *plus* FIGURE-8 *ring implementation*

1. Basic proposal

The proposed first step toward detecting T-violation is to keep in place the right arc of the present racetrack-shaped COSY ring, shown in Fig. 5, completing it with the present left arc of COSY (moved from its current location at the left end of the COSY beam hall) to complete a nearly circular bunch accumulator BA or, if one prefers, the right arm of FIGURE-8. This would make room for the PTR ring, or if one prefers, the left arm of FIGURE-8, (the need for which is explained and justified in the CYR[23] as a prototype for an all-electric, full-scale, nominal, proton EDM measurement ring.

As described in the CYR, the first, and most important PTR challenge is to produce a storage ring having superimposed magnetic and electric bending needed to freeze proton spins. The second major challenge is to demonstrate simultaneously circulating proton beams, as needed for ultimate proton EDM measurement precisions. This capability is secondary in importance only because the EDM measurement can proceed use beams that circulate consecutively rather than concurrently.

Subsequent to the CYR it has been realized, for example as explained reference [42] and in the present paper, that PTR can, itself, be used for multiple tests of time reversal symmetry, at least one of which, the d-EDM measurement, is much easier than the p-EDM measurement. T-symmetry can also be tested in low energy elastic pp or dd scattering.

2. Challenges and sensible design principles

For most accelerator projects the greatest risk of failure concerns the possible failure to achieve sufficient injection efficiency. It was failure to protect against this risk that was responsible for the failure of the SSC Supercollider in the U.S.A. This risk applies to every commissioning step in the sequence of steps just described in the previous subsection.

Success probability of any accelerator project is greatly improved by another principle; success is best assured by using previously-commissioned components. The best evidence for the validity of this principle comes from its frequent successful application at CERN, the most recent being the success of the LHC. The best example of project failure caused by failure to respect this principle comes also from the SSC, in the form of the failure to recognize that moving the site from Fermilab to Texas, was tantamount to discarding a large fraction of the needed equipment and irreplaceable experience.

A restatement of this principle in simpler terms is that, just because something has been done somewhere in the past, does not necessarily make it easy to replicate in the present. This applies explicitly to several capabilities that have been developed, or improved at COSY. These include stripper injection with polarization preservation, including debunching and rebunching into nearly 100% polarized bunches, electron cooling, stochastic cooling, phase-locked spin control, MDM measurement of sufficient numerical precision to enable the setting and resetting conditions with accuracy greater than can be achieved by measuring electric and magnetic fields.

3. Project sequencing and risk

It is indisputable that what is being proposed in this paper is very complicated; far too complicated for the sequencing to be spelled out in detail. Discussion here is limited to the application of principles just described to a few decision points that are certain to come up as the project proceeds. Physical realities make it impossible to avoid all risk, but it is advisable to take only risks that are unavoidable.

1. There is one risk over which experimentalists have only a single control. It is the risk of losing financing, with past success being the only control.

2. The deuteron EDM proposal in the present paper is significantly more complicated than the ingenious Senichev deuteron EDM configuration shown in Figure 10. For that design there is no risk associated with injection—the existing COSY ring could serve as injector. Under ideal circumstances a d-EDM determination in the Senichev"ring" would likely be competitive with a d-EDM determination in PTR. But circumstances are rarely ideal and, once the bending elements are in place, the Senichev design has zero flexibility. The separate electric and magnetic arcs constrain the electric to magnetic field ratio uncontrollably, which makes success unlikely.

   It is the superposition of electric and magnetic bending that overcomes this limitation, and justifies the risk associated with extra complication.

3. As shown in Figure 5, the overall length of the proposed complex slightly exceeds the available internal COSY beam hall length. One option would be to extend the building slightly. Another would be to shrink the design bending radii of both rings by roughly three percent to reduce the complex length by roughly three meters (while retaining all the same beam line elements).

   Either option would be quite straightforward. All injection infrastructure and electron cooling, essentially unchanged from at present, could then be recommissioned and used to develop and test procedures for the tailoring of individualized bunch polarizations. In this way, the bunch accumulator BA, or if one prefers, the right arm of FIGURE-8 could be swiftly restored to operation, with purely magnetic bending.

The problem with the previous paragraph is that it under-estimates the risk to injection, extraction, and cooling associated with any unnecessary mechanical tinkering with sectors of COSY that contain injection, extraction, or electron cooling components.

There is little doubt that these risks outweigh the cost of extending the COSY beam hall.

4. There is *unavoidable* injection risk associated with moving the present left arc of COSY to complete bunch accumulator BA.

   One might argue that all-magnetic bends should be replaced by EM-bends at this time, as required by the eventual exploitation of spin-transparency for the deuteron-EDM capability, which requires all FIGURE-8 bends to have superimposed electric and magnetic bends (EM-bends).

   This is wrong for a few reasons. It would impose uncontrollably long delay associated with the uncertain development of EM-bending, and it would violate the principle that fragile injection components must not be touched.

   More fundamentally important is that the successful implementation of spin-transparency capability in FIGURE-8 does not, in fact, require left-right symmetry of left and right arms of FIGURE-8. It is top-bottom symmetry (in the figure) that must be maintained. With only EM-bends in the left arm one needs to some some, but not necessarily all bends with EM-bends in the right arm of FIGURE-8; the EM-bend replacements must be up-down symmetric to retain spin-transparency functionality.

   In the Senichev design (and in his terminology) because of the small deuteron MDM, *the beam only needs to have quasi-frozen spins(QFS) to preserve EDM sensitivity.* The transverse run-out of a nominally forward pointing EDM in an electric arc is canceled in the adjacent magnetic arc.

   For our EDM measurement two solenoid Siberian half-snakes will be required in each beam crossover line, to preserve already-established out-of-plane EDM-induced precession. However, the separate partial rings must also have separately vanishing (or, at least, matched) spin tunes. Otherwise, transverse polarization errors entering the crossover region would be reversed by the Siberian snakes, only to be further amplified by the subsequent opposite sign bending.

   In our design any non-zero spin tune increment acquired in the left arm of FIGURE-8 can be compensated in the right arm, but only if some sectors of the right arm contain (adjustable) EM-bends, and they are top-bottom symmetric (in the figure). This meets the requirements that both full-ring and half-ring spin tunes vanish.

   The only penalty this imposes is to require the electric field strengths to be increased (from the low value that makes the deuteron-EDM measurement so attractive). This makes it appropriate to replace as many all-magnetic bends as possible, consistent with their containing no fragile elements and preservation of top-bottom FIGURE-8 symmetry.

   Of the 16 natural sectors in two rings, four disappear in favor of cross-overs, leaving six active sectors in each arm of FIGURE-8. All six sectors in the left arm will contain EM-bends while, let us say, just two fragile sectors in the right arm need to remain all-magnetic. Then, the excess spin tune shift in ten sectors would have to be compensated in four sectors, causing the electric field to be correspondingly stronger.

5. Having deferred tampering with fragile injection sectors through the entire construction period to this point, one will, eventually, risk losing injection capability temporarily, as a result of replacing all remaining all-magnetic bends by EM-bends, and carefully restoring the sensitive components.

6. Eventually, all needed components and sectors will have been completed and installed to support the compatible existence of both FIGURE-8 collider functionality and the circular PTR + BA EDM capability contemplated in recent PTR planning reports. Though these two modes of operation are compatible, they could obviously not work at the same time.

   Here "compatible" is being used loosely. Realistically, quite long shutdown periods have to be anticipated for the conversion of FIGURE-8 to or from PTR + BA. With careful organization it should be possible to alternate construction and commissioning periods without incurring very much excess delay.

7. *The motivation for considering a figure-eight shape derives from the requirement to enhance T-violation in elastic scattering (with acceptably small impact on its eventual role as EDM prototype ring). However the capability to freeze proton spins to* $Q_S = 0$ *must be, and will be being preserved during the proposed construction sequencing. Eventually, small rearrangements can convert the arm on the right to beam accumulator (BA), and the ring on the left to the currently envisaged PTR design; compare Figure 5* with Figure 5 of reference [2].

   For the circular lattice EDM sensitivity to be carried over to the figure-eight shape it is, of course, necessary for the overall spin tune to vanish. Following the Derbenev et al, prescriptions[3], this is permitted by the figure-eight configuration, as has been described.

8. In summary, one notes that the complication associated with addressing EDMs and elastic scattering together has not increased the most serious risk to the enterprise, namely injection. To the contrary, as well as minimizing the injection risk it has limited the risk associated with the lack of enthusiasm for working on a project that is only a prototype for a project likely subject to interminable delay, because of its high cost.

Appendix A: Relativistic elastic scattering kinematics

The historically-conventional dynamical variable specifying incident beam energy for fixed target experiments was the laboratory energy $K_{lab}^{ft-equiv}$. The "ft-equiv" superscript serves as a reminder that $K_{lab}^{ft-equiv}$ is not the same as K_{lab} for a particle in a storage ring. For comparison with historical data it is useful to have a formula giving $K_{lab}^{ft-equiv}$ in terms of K_{lab} which is the laboratory kinetic injection energy of a stored beam.

For relating kinematics in parallel traveling reference frames it is convenient to introduce s as the square of the rest frame (total) energy of the two particle state:

$$s = 4\big((m_pc^2)^2+(p'_pc)^2\big), \quad \text{or} \quad s = 2m_pc^2(2m_pc^2+K_{lab}). \tag{A1}$$

where p'_p is the CM momentum. Inverting the first of these

$$p'_pc = \sqrt{s/4 - m_p^2c^4}. \tag{A2}$$

Then the "equivalent", fixed target kinetic energy is given in terms of the stored beam kinetic energy, by

$$K_{lab}^{ft-equiv} = \frac{s-2(mc^2)^2}{2mc^2} - mc^2. \tag{A3}$$

Though relativistically exact, these formulas may seem to be unduly complicated; approximating the scattering as non-relativistic might be considered as a sensible first approximation. As it happens, though, the approximate constancy implied by Eq. (11) greatly simplifies the application of the fully relativistic formulation.

Because the scattering is isotropic in the CM, the energy distributions are uniform also in the laboratory. This is academic in our case of equal energy, orthogonal collision in the laboratory, since all energies, incident and scattered, are identical.

Appendix B: Protons slowing and stopping in graphite

From Fig. 3 one sees, in right angle crossing collision geometry, that the laboratory frame is close to, but not quite equal to the center of mass (CM) frame. Nevertheless, in our orthogonal collision geometry, compared to laboratory fixed target scattering measurement, scattering symmetries are much better preserved. The horizontal, x, y, and vertical x, z planes are common to both laboratory and CM frames, thereby preserving left/right and up/down symmetries. Though elastically scattered protons are exactly collinear in the CM frame, they are more nearly orthogonal in our laboratory frame.

To simplify discussion, we will ignore the implied slow transverse velocity of the laboratory, taking it as the CM frame. In this approximation, all CM scatters through $\pi/2$ lie in the same "orthogonal" plane, common to laboratory and CM frames and have azimuthal angles preserved, but polar angles are slightly distorted. Scattered particles have identical energies but not collinear paths.

Table V shows stopping powers and ranges for kinetic energies in the applicable range. With graphite density of $1.7\,\mathrm{g/cm^2}$, all 80 MeV protons will stop in 4 cm of graphite, producing accurate energies for all scattered protons. Precision energy determination (for example to exclude inelastic scatters) depends on the full stopping range. But, since the p, C polarization analyzing power falls with decreasing proton energy, polarimetric analyzing power is provided mainly by the left/right asymmetry of p, C elastic scatters in the first half of their ranges, while their energies exceed 50 MeV.

K.E.	Stopping Power MeV cm^2/g			range gm/cm^2
MeV	electronic	nuclear	total	
20	23.31	1.006E-02	23.32	0.4764
40	13.31	5.221E-03	13.31	1.664
60	9.642	3.553E-03	9.645	3.457
80	7.714	2.703E-03	7.717	5.794

TABLE V. Stopping power for protons stopping in graphite, density $1.7\,\mathrm{gm/cm^2}$. NIST[43]

Since neutron and proton cross sections are approximately equal in this energy range, the nuclear scattering efficiency and quality can be assessed from the neutron/carbon scattering data shown in Fig. 12. This shows that most of the nuclear scatters occurring in the graphite plates provide useful analyzing power.

Appendix C: Luminosity and data rates

Because of the crossover sections of FIGURE-8, its design circumference $\mathcal{C}_{\mathrm{fig8}}$ is somewhat greater than the circumference of BA, which is $C_0 = 102.5\,\mathrm{m}$, with mean radius $102.5/(2\pi)$. $\mathcal{C}_{\mathrm{fig8}}$ can be determined from

$$C_{\mathrm{fig8}} = 2\Big(\frac{3}{4}C_0 + 2\frac{C_0}{2\pi}\Big) = 102.5 \times 2.13 = 219\,\mathrm{m}. \tag{C1}$$

For beam energy of 80 MeV, $\gamma = 1.082$, $\beta = 0.381$, $v = \beta c = 1.143 \times 10^8\,\mathrm{m/s}$. The revolution period is $T_0 = 1.916\,\mu\mathrm{s}$, and the revolution frequency is $f = 0.522\,\mathrm{MHz}$.

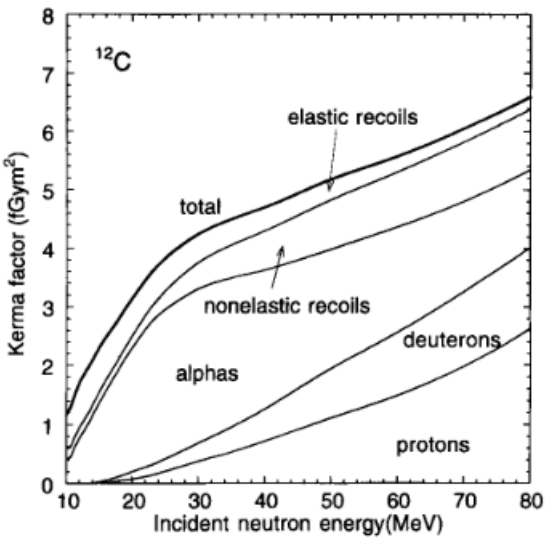

Fig. 19 Calculated partial kerma factors for each emitted particle and elastic and nonelastic recoils

FIG. 12. Primary reaction processes of the n+ 12 C reaction considered in the present evaluation. Photo-copied from reference [44], including the figure caption from that paper.

Sands[45], Eq. (1.17), gives the total luminosity for 2 circulating bunches in a circular ring

$$\mathcal{L}_{\rm circular} = \frac{f}{4}\,\frac{N_p^2}{A_{\rm int}} \tag{C2}$$

where N_p is the number of protons in each bunch, and $A_{\rm int}$ is an effective interaction area.

Assuming the beam shapes are Gaussian, the rms beam standard deviations σ_x and σ_y can be inferred from the emittances $\epsilon_x(P_h)$ and $\epsilon_y(P_h)$, where the parameter P_h, a number in the range from 0 to 1, specifies the fraction of all particles contained within the specified emittance. They are related by the equation,

$$\epsilon(P_h) \equiv \frac{\epsilon_{\rm invariant}(P_h)}{\gamma} = -2\pi\ln(1-P_h)\,\frac{\sigma^2}{\beta}. \tag{C3}$$

For the special choice P_h=0.14714, one obtains $\epsilon(0.14714)$=σ^2/β. This relation permits the Gaussian standard deviation σ to be evaluated at a position in the ring at which the lattice function β is known. Taking $\epsilon_{n,95} = 5\,\mu$m as a tentative normalized emittance containing 95 percent of the particles, with $\beta = 0.0.381$ and $\gamma = 1.082$, this corresponds to "geometric" emittance

$$\epsilon_{95} = \frac{\epsilon_{n,95}}{\beta\gamma} = 12.1\,\mu{\rm m}. \tag{C4}$$

[13] "Short" bunches are short compared to the beta functions at the

Alexei Fedotov[46] states that 95 percent transverse emittances and r.m.s. emittances are related by $\epsilon_{95} = 6\epsilon \equiv 6\sigma^2/\beta$. At the collision point, with $\beta_x = \beta_y = \beta^*$, the beam standard deviations are

$$\sigma^* \approx \sqrt{\beta^*\epsilon_{95}/6} \quad \Big(\stackrel{\rm e.g.}{=} \sqrt{0.1\times 19.6\times 10^{-6}/6} = 0.449\,{\rm mm}\Big). \tag{C5}$$

With head-on collisions of short bunches[13] The effective crossing area is the same as the bunch transverse area, which Sands[45], Eq. (6.2) gives as

$$A_{\rm int} = \pi\sigma_x\sigma_y = 0.634\times 10^{-6}\,{\rm m}^2. \tag{C6}$$

For luminosity calculation we assume the IP beta function values are $\beta_x^* = \beta_y^* = 0.1\,$m.

There are two major deficiencies in the luminosity formulas written so far. The more important defect is that the formulas apply to head-on collisions, not to our orthogonal figure-8 collisions. Since we do not have enough information to rectify this defect, we defer its discussion. As discussed elsewhere, the present paper concentrates on obtaining optimal statistical procedures, rather than on calculating the achievable absolute precision with which fractional T-violation can be measured.

The lesser deficiency is that circular, rather than figure-8 geometry has been assumed For circular geometry the CERN Yellow Report has taken N_p, the number of stored particles in PTR, as limited by intra-beam scattering, to be 2×10^{10}, with $N_p = 10^{10}$ particles per bunch. (Though not very reliable, itself) we accept the result, neither doubling the luminosity to account for reduced IBS from the doubled circumference, nor cutting N_p in half to account for the doubled number of bunches.

Note, though, that Sands (assuming a single IP) has one collision per revolution, while we have four collisions per revolution, albeit at half the frequency. Since the frequency is accounted for explicitly, the figure-8 luminosity is given by

$$\mathcal{L}_{\rm fig8} = f\,\frac{N_p^2}{A_{\rm int}} = \frac{0.522\times 10^6\times 10^{20}}{0.634\times 10^{-6}\times 10^4} \approx 10^{28}\,{\rm cm}^{-2}{\rm s}{-}1. \tag{C7}$$

where the extra denominator factor of 10^4 accounts for the luminosity being quoted in its customary c.g.s. units. This luminosity can also be quoted as 10 inverse millibarns per second.

Using the total elastic scattering cross section $\sigma = 21.3\,$mb, given in Eq. (10), multiplying this by the luminosity given in Eq. (C7), and assuming every scatter within the apparatus acceptance is counted during data collection over a "nominal year" of $10^7\,$s, gives the total expected rate of detected scatters to be

$$\text{detected scatters} \approx 2\times 10^9 \text{ per nominal year.} \tag{C8}$$

[1] R. Talman, *Superimposed Electric/Magnetic Dipole Moment Comparator Lattice Design,* ICFA Beam Dynamics Newsletter #82, Yunhai Cai, editor, Oct, 2021

[2] R. Talman, *Difference of measured proton and He3 EDMs: a reduced systematics test of T-reversal invariance,* submission JINST_060P_0522 for publication in the Journal of Instrumentation, May, 2022

[3] Y.S. Derbenev et al., *Siberian Snakes, Figure-8 and Spin Transparency Techniques for High Precision Experiments with Polarized Hadron Beams in Colliders,* Symmetry, 13, 398. https://doi.org/10.3390/sym13030398, 2021

[4] T.D.Lee and L. Wolfenstein, *Analysis of CP-Invariant Interactions and the K_1^0 and K_2^0 system,* Phys. Rev. **138**, 68, 1965

[5] J. Prentki and M. Veltman, *Possibility of CP violation in semi-strong interactions,* Phys.Letters15,88, 1965

[6] L. B. Okun, *Remark on CP-parity,* Sov. J. Nucl. Phys., **1**, 1965

[7] I.Yu. Kobzarev, L.B. Okun et al., *The Violation of CP Invariance,* https://doi.org/10.1070/PU1967v009n04ABEH003013

[8] J. Blatt and V. Weisskopf, *Theoretical Nuclear Physics,* Dover Publications, 1991 reprint of Springer-Verlag, 1979, from John Wiley, 1952

[9] G. Gamow and C. Critchfield, *Theory of Atomic Nucleus and Nuclear Energy Sources,* Scholar Select reprint of Oxford, at the Clarendon Press, 1949

[10] J. Bystricky, F. Lehar, and P. Winternitz, *On tests of time reversal invariance in nucleon-nucleon scattering,* Journale de Physique, **45**, 2, pp 207-224, 1984

[11] C. Lechanoine-LeLuc and F. Lehar, *Nucleon-nucleon elastic scattering and total cross sections,* Rev. Mod. Phys, **65**, 1, 1993

[12] N. Mott and H. Massey, *The Theory of Atomic Collisions,* Oxford, at the Clarendon Press, p391, 1965

[13] S.D. Drell and A.C.Hearn, *Exact sum rule for nucleon magnetic moments,* Phys. Rev. **16**, 20, 1965

[14] S.B. Gerasimov, Sov. J. Nucl. Phys. 2 430, 1966

[15] K. Helbing, *Experimental verification of the GDH sum rule,* arXiv:nucl-ex/0603021v3 29 Mar 2006, and Physikalisches Institut, Universitat Erlangen-N, 2018

[16] C. Wilkin, *The legacy of the experimental hadron physics program at COSY,* Eur. Phys. J. A 53 (2017 114, 2017

[17] D. Eversmann et al., *New method for a continuous determination of the spin tune in storage rings and implications for precision experiments,* Phys. Rev. Lett. **115** 094801, 2015

[18] N. Hempelmann et al., *Phase-locking the spin precession in a storage ring,* P.R.L. 119, 119401, 2017

[19] F. Rathmann, N. Nikoliev, and J. Slim, *Spin dynamics investigations for the electric dipole moment experiment,* Phys. Rev. Accel. Beams 23, 024601, 2020

[20] J. Slim et al., *First detection of collective oscillations of a stored deuteron beam with an amplitude close to the quantum limit,* Phys. Rev. Accel. Beams, 24, 124601, 2021

[21] F. Rathmann, *First direct hadron EDM measurement with deuterons using COSY,* Willy Haeberli Memorial Symposium, https://www.physics.wisc.edu/haeberli-symposium, 2022

[22] R.Talman, *Improving the hadron EDM upper limit using doubly-magic proton and helion beams,* arXiv:2205.10526v1 [physics.acc-ph] 21 May, 2022

[23] CPEDM Group, *Storage ring to search for electric dipole moments of charged particles Feasibility study,* CERN Yellow Reports: Monographs, CERN-2021-003, 2021

[24] R. Talman and N. N. Nikolaev, *Colliding beam elastic pp and pd scattering to test T- and P-violation,* Snowmass 2021, Community Town Hall/86, 5 October, 2020

[25] P. Lenisa et al., *Low-energy spin-physics experiments with polarized beams and targets at the COSY storage ring,* EPJ Techniques and Instrumentation, https://doi.org/10.1140/epjti/s40485-019-0051-y, 2019

[26] N. Mott and H. Massey, *The Theory of Atomic Collisions,* Oxford, at the Clarendon Press, 1965

[27] M. Han and Y. Nambu, *Three-Triplet Model with Double SU(3) Symmetry,* Phys. Rev. **129**, 4B, 1965

[28] A.D. Sakharov, *Violation of CP invariance, C asymmetry, and baryon asymmetry of the universe,* JETP Lett. **5**, 24-27, 1967

[29] F. Arash, M. Moravcsik, and G. Goldstein, *Dynamics-independent Null, experiment for testing time-reversal independence,* Phys. Rev. Lett., **54**, 2649, 1985

[30] L. Stodolsky, Nucl. Phys., *Parity violation in threshold neutron scattering,* **B197**, 213, 1982

[31] Yu.N. Uzikov and A.A. Temerbayev, *Null-test for T-invariance violation in pd scattering,* arXiV:1506.08303v1 [nucl-th] 2015

[32] A. Abashian and E. M. Hafner. *Experimental test of time-reversal invariance in strong interactions,* Phys. Rev. Lett. **1**, 7, p. 255, 1958

[33] C.A. Davis et al., *Test of time reversa1 invariance in p-p elastic scattering at 198.5 MeV.* Phys. Rev. C, **33**, 4, 1986

[34] E. Aprile et al. *Upper Limit for T-Invariance Violation in Elastic pp Scattering,* Phys. ReV. Lett. **47**, 19, 1981

[35] H. Bethe and P. Morrison, *Elementary Nuclear Theory,* Dover republication, 1906, of Second Edition, John Wiley & sons, 1956

[36] M. Iberaku et al., *Measurements of elastic scattering and total non-elastic cross sections for 40-80 MeV neutrons at TIARA,* JAERI-Conf 2000-005

[37] M. Ieira, et al., *A multifoil carbon polarimeter for protons between 20 and 84 MeV,* Nuclear Instruments and Methods in Physics Research, **A257**, 253-278, 1987

[38] Z. Bagdasarian et al., *Measurement of the analysing power in proton-proton elastic scattering at small angles,* Physics Letters B, **739**, 152, 2014

[39] Y.S. Derbenev et al., *Polarization preservation and control in a figure-8 ring,* International Journal of Modern Physics: Conference Series Vol. 40 1660090, 2016

[40] Y. Filatov et al. *Transparent spin method for spin control of hadron beams in colliders,* Phys. Rev. Lett., 124, 194801, 2020

[41] C. Weidemann et al., *Toward polarized antiprotons: Machine development for spin-filtering experiments*, Phys.Rev.ST Accel.Beams 18, 2, 020101, 2015

crossing point. In low energy pp and p,d elastic scattering experiments the bunches may be too long to meet this condition. This would reduce the luminosity, but we ignore this complication.

[42] Yu. Senichev, *Quasi-frozen spin method for EDM deuteron search,* doi10.18429/JACoW-IPAC2015-MOPWA044, 6th International Particle Accelerator Conference, Richmond, VA, USA, 2015

[43] National Bureau of Standards Physical Measurement Laboratory, https://physics.nist.gov ⟩ PhysRefData ⟩ Star ⟩ Text

[44] S Chiba and T Fukahori, *Evaluation of Neutron Cross Sections of Carbon-12 for Energies up to 80 MeV,* Journal of NUCLEAR SCIENCE and TECHNOLOGY, Vol. 34, No.2 1997

[45] M. Sands, *The Physics of Electron Storage Rings, in Internaional School of Physics, "Enrico Fermi",* Academic Press, 1971

[46] A. FedotovPrivate communication